

THE DYNAMIC YIELDING OF MILD STEEL

THE DYNAMIC YIELDING OF MILD STEEL

BY

KALYAN HARPALANI

A Thesis

Submitted to the Faculty of Graduate Studies

in Partial Fulfilment of the Requirements

for the Degree

Master of Engineering

McMaster University

May, 1969

MASTER OF ENGINEERING (1969)  
(Mechanical Engineering)

McMASTER UNIVERSITY  
Hamilton, Ontario.

TITLE: The Dynamic Yielding of Mild Steel

AUTHOR: Kalyan Harpalani, B.Tech (Mech. Eng.)

I.I.T., Kanpur, India.

SUPERVISER: Dr. G. Kardos

NUMBER OF PAGES: x, 90

SCOPE AND CONTENTS:

Dynamic stress tests were performed on mild steel samples. The material parameters ' $n$ ' and ' $G(\epsilon_r, t_0)$ ', defined as 'stress dislocation velocity exponent' and 'flow function' respectively, were evaluated using the equation " $\sigma_m^n t_0 K(n) = G(\epsilon_r, t_0)$ " as proposed by Kardos (1). The values determined for ' $n$ ' are in agreement with the results obtained by other researchers using different techniques.

The equipment for studying the response of materials to dynamic loading was modified to permit a wider duration range for the loading.

A technique was developed to monitor the pressure of the oil in the intensifier throughout the entire loading cycle.

### ACKNOWLEDGEMENTS

The author wishes to express his appreciation to Dr. G. Kardos for his continuous encouragement and invaluable suggestions made during the course of this work.

The author is thankful to the workers of the machine shop of McMaster University for fabricating various parts of the equipment, and preparing samples for the present test.

The author also wishes to acknowledge the assistance offered by the technicians of the Large Scale Experimental Building in setting up the equipment.

The present work was supported under N.R.C. Grant No. A3340.

## TABLE OF CONTENTS

	PAGE
ACKNOWLEDGEMENTS	iii
TABLE OF CONTENTS	iv
LIST OF ILLUSTRATIONS	vi
NOMENCLATURE	viii
1. <u>INTRODUCTION</u>	1
2. <u>TEST PROGRAM</u>	
2.1 Brief Description of Test Apparatus	7
2.2 Test Objectives	8
2.3 Test Procedure	12
2.4 Test Results	14
3. <u>DISCUSSION AND CONCLUSIONS</u>	
3.1 Dynamic Response of Mild Steel	20
3.2 Correlation with Theory	21
3.3 Correlation between Nominal Peak Stress and Residual Strain	21
3.4 Flexibility of the Tester	22
3.5 Monitoring the Pressure Pulse	23
3.6 Recommendations for Future Work	23

## APPENDICES

I. <u>ANALYSIS OF THE SYSTEM</u>	
I.1 Elasticity of the System	24

I.2	Response of the Strain Gage	28
II.	<u>EVALUATION OF THE RESULTS</u>	
II.1	Determination of Stress-Time Function	29
II.2	Determination of 'n'	30
II.3	Evaluation of Flow Function	36
II.4	Estimation of Energy Dissipated in Yielding	36
III.	<u>ANALYSIS FOR DETERMINING RELATION BETWEEN NOMINAL PEAK STRESS AND RESIDUAL STRAIN</u>	38
IV.	<u>TABLES</u>	43
V.	<u>FIGURES</u>	63
	<u>REFERENCES</u>	90

## LIST OF ILLUSTRATIONS

FIGURE	PAGE
1. General View of the Experimental Set Up	64
2. The Strain Gage Cemented to the Wall of the Intensifier	65
3. Wilder Micro Projector	65
4. Pressure Transducer Connected to the Lower Portion of the Intensifier	66
5. Pressure Transducer Connected to the Intensifier through the Air-Vent	66
6. Pressure Pulse Obtained from the Configuration Shown in Figure 4	67
7. Pressure Pulse Obtained from the Configuration Shown in Figure 5	67
8. Load-Time Trace for the Test Sample 1610	68
9. Load-Time Trace for the Test Sample 169	68
10. Load-Time Trace for the Test Sample 165	69
11. Load-Time Trace for the Test Sample 166	69
12. Load-Time Trace for the Test Sample 258	70
13. Load-Time Trace for the Test Sample 256	70
14. Sectional View of the Intensifier	71
15. Stress Pulse for Constant Rate of Loading	72
16. Stress Pulse for an Ideally Elastic-Plastic Material	72
17. Plots of Peak Load versus Drop Height	73

18.	Nominal Peak Stress versus Residual Strain- Batch A	74
19.	Nominal Peak Stress versus Residual Strain - Batch B	75
20.	Loading Duration versus Apparent Dynamic Yield Stress - Batch A	76
21.	Peak Stress versus Residual Strain - Batch A	77
22.	Peak Stress versus Residual Strain - Batch B	78
23.	Rate of Strain versus Yield Stress - Batch A	79
24.	Rate of Strain versus Yield Stress - Batch B	80
25.	Flow Function versus Residual Strain - Batch A	81
26.	Flow Function versus Residual Strain - Batch B	82
27.	Mass of the Drop Table versus Loading Duration	83
28.	Peak Load versus Mass of the Drop Table	84
29.	Residual Strain versus Energy Dissipated in Yielding - Batch A	85
30.	Residual Strain versus Energy Dissipated in Yielding - Batch B	86
31.	Theoretical Derived Curves, Illustrating the Correlation between Nominal Peak Stress and Residual Strain	87
32.	Residual Strain versus Energy Dissipated in Yielding - Batch A	88
33.	Residual Strain versus Energy Dissipated in Yielding - Batch B	89

## NOMENCLATURE

$A_1$	Area of test specimen
$A_2$	Area of loading piston
$A_3$	Area of drive piston
$B$	Bulk modulus of oil
$\beta$	Proportionality constant
$C$	Number of dislocations which should be released to produce yield
$C_1$	Constant
$C_2$	Proportionality constant
$C_3$	Proportionality constant
$\Delta$	Difference operator
$E$	Young's modulus of elasticity
$\epsilon_p$	Plastic strain
$\epsilon_r$	Residual strain
$\epsilon_y$	Plastic strain at yield point
$\dot{\epsilon}$	Rate of strain
$f(t/t_0)$	Time function defined by the equation, $\sigma(t) = \sigma_m f(t/t_0)$
$\phi$	Time ratio $t/t_0$
$g$	Acceleration due to gravity
G.F.	Gage factor for strain gage
$G(\epsilon_r, t_0)$	Flow function corrected for strain hardening
$H$	Drop height for the falling table

$H(\epsilon_r)$	Flow function
$K(n)$	Form function
$L$	Length of bolts of the intensifier
$L_1$	Length of test specimen
$M$	Mass of the drop table
$n$	A material constant known as Stress Dislocation Velocity Exponent
$P$	Pressure of oil in the intensifier
$q$	Strain hardening coefficient
$R$	Resistance of an arm of the wheatstone bridge
$r$	Internal radius of cylindrical wall of the intensifier
$\sigma_e$	Maximum stress for elastic test
$\sigma_m$	Maximum stress for the test on soft sample
$\sigma_y$	Yield stress
$\sigma_0$	Constant
$\sigma(t)$	Stress-time function
$t$	Time
$t_e$	Duration of loading for elastic test
$t_E$	Duration of loading if the bulk modulus of oil used in the intensifier were infinite
$t_0$	Duration of loading for test sample
$t_y$	Period elapsed before reaching yield point
$t_\infty$	Pulse duration for an infinite value of the system elasticity
$v$	Volume of oil in the intensifier

V            Excitation voltage for transducer  
W            Spring constant for intensifier  
x            Displacement of drive piston

## CHAPTER 1

### INTRODUCTION

It has long been known that some engineering materials exhibit greater strength under dynamic loading. This fact was first realised by J. Hopkinson (3) in 1872. While studying the propagation of elastic waves in solids, he observed that rupture occurred at stresses higher than those predicted by static tests. Most of the experimental work in this area has been done after the Second World War, which provided impetus to the study of the dynamic properties of materials, in particular with respect to impact and high rate metal forming. A review of the work done in this field is presented in References 1 and 9.

The present study is related to the response of materials subjected to impulsive loadings. A technique has been developed to predict the behaviour of materials under short time loadings. The original theoretical and experimental investigations in this area were carried out by G. Kardos (1). His theoretical investigation was an extension of the work done by Hahn (4). The design equation derived in Reference 1 is as follows:

$$\int_0^{t_0} (\sigma(t) - q_{ep})^n dt = H(\epsilon_r) \quad \text{--(1.1)}$$

The equation contains three material constants.

$q$  = Strain Hardening Coefficient

$n$  = Stress Dislocation Velocity Exponent

$H(\epsilon_r)$  = Flow Function

The value of the flow function depends upon the material and the magnitude of the residual strain. In the equation,  $\sigma(t)$  is the stress function and  $\epsilon_p$  is the instantaneous value of the plastic strain.

By limiting the region of application to small plastic strains, i.e., in the order of 0.1 percent, the strain hardening term can be omitted and equation (1.1) simply becomes

$$\int_0^{t_0} (\sigma(t))^n dt = H(\epsilon_r) \quad \text{--(1.2)}$$

This simplified design equation only requires the determination of two dynamic material functions. It is interesting to observe that this equation is mathematically identical to the yield criterion proposed by Campbell (5) for mild steel. Campbell's equation is given by

$$\int_0^{t_0} (\sigma(t)/\sigma_0)^n dt = C \quad \text{--(1.3)}$$

where  $\sigma_0$  is a constant and  $C$  is the number of

dislocations, which should be released to produce yield.

For higher values of the plastic strain, the strain hardening term in equation (1.1) cannot be neglected. For such cases, Kardos (1) proposed the following relation:

$$\int_0^{t_0} (\sigma(t))^n dt = G(\epsilon_r, t_0) \quad \text{--(1.4)}$$

where  $G(\epsilon_r, t_0)$  is the value of the flow function corrected for strain hardening. The function depends on both the residual strain and the duration of loading.

The application of the above equation can be simplified by normalizing it in order to separate the variables. The equation can be expressed in the following form:

$$\int_0^{t_0} (\sigma(t))^n dt = (\sigma_m)^n t_0 \int_0^1 (f(\phi))^n d\phi \quad \text{--(1.5)}$$

$$\text{where } \phi = t/t_0$$

$$\sigma(t) = \sigma_m f(t/t_0)$$

$$\sigma_m = \text{Peak Stress}$$

The integral on the right hand side of the equation

depends upon the form of the stress pulse, and is known as 'Form Function'. Equation (1.4) can now be presented in the following form:

$$(\sigma_m)^n t_0 K(n) = G(\epsilon_r, t_0) \quad \text{--(1.6)}$$

where  $K(n) = \text{Form Function}$

The values of the flow function and 'n' can be determined experimentally and the results can be used to predict the amount of the plastic strain corresponding to any particular stress function.

Equation (1.2) can be used to obtain a relation between rate of strain and the yield stress. Assuming the stress function to be a ramp pulse (Figure 15), yielding will occur when

$$\int_0^{t_y} (\sigma(t))^n dt = C_1 \quad \text{--(1.7)}$$

where  $C_1$  is the value of the flow function corresponding to the plastic strain at the yield point, and  $t_y$  is the time required to produce yield. Since the value of the plastic strain corresponding to yield point is very low, the

value of the flow function can be assumed to be a constant, independent of the duration of loading.

As there is a linear relationship between stress and time, equation (1.7) reduces to

$$(\sigma_y)^n t_y / (n+1) = C_1 \quad \text{--(1.8)}$$

where  $\sigma_y$  = Yield Stress

$1/(n+1)$  = Form Function for a Ramp Pulse

For this stress function, the rate of strain is constant and is given by

$$\dot{\epsilon} = (\sigma_y) / (E t_y) \quad \text{--(1.9)}$$

By eliminating 't<sub>y</sub>' from equations (1.8) and (1.9), the following relation may be obtained:

$$(\sigma_y)^{n+1} = C_2 \dot{\epsilon} \quad \text{--(1.10)}$$

where  $C_2 = C_1 E (n+1)$

Equation (1.10) can be rewritten in the following form:

$$\sigma_y = C_3 (\dot{\epsilon})^{1/(n+1)} \quad \text{--(1.11)}$$

where  $C_3 = (C_2)^{1/(n+1)}$

Biggs (8) in discussing high strain rates and brittle fracture quotes Hollmans' proposed relationship for strength at high strain rates.

$$\sigma = \beta (\dot{\epsilon})^n \quad \text{--(1.12)}$$

where  $\sigma =$  Stress at failure

$\beta, n =$  Material Constants

It is interesting to note that equation (1.11) is mathematically identical to equation (1.12).

## CHAPTER 2

### TEST PROGRAM

#### 2.1 Brief Description of the Test Apparatus

A general view of the experimental set up is given in Figure 1. The test equipment mainly consists of a drop table and a hydraulic intensifier. The equipment can be used to subject a material specimen to a loading cycle which very nearly approximates a half sine curve. The peak load and the duration of the loading pulse can be varied independently by changing the volume of the oil in the intensifier and the mass of the drop table. A detailed description of the equipment is given in References 1 and 2.

The main features of the equipment may be briefly stated as follows:

- (a) The material specimen is subjected to only a single loading cycle.
- (b) The loadings are measured directly and monitored throughout the entire loading cycle.
- (c) The magnitudes of the load and the pulse duration are independently variable.
- (d) The induced stress is a simple direct stress on a standard test specimen.

## 2.2 Test Objective

The main objectives of the present work are outlined as follows:

- (i) To study the response of mild steel samples to dynamic loading.
- (ii) To modify the equipment so as to permit a wider range of pulse durations.
- (iii) To monitor the pressure of the oil in the intensifier throughout the entire loading cycle.

For obtaining better results, it is necessary that the material specimens should be tested under loading cycles with a wide range of pulse durations. The test apparatus analysis in Reference 1 shows that the stress pulse obtained from the equipment can be expressed as:

$$\sigma(t) = (A_2/A_1)\sqrt{2BHMg/v} \sin(A_3\sqrt{B/Mv})t \quad \text{--(2.2.1)}$$

where

$A_1$  = Area of the specimen

$A_2$  = Area of the loading piston

$A_3$  = Area of the drive piston

$g$  = Acceleration due to gravity

M = Mass of the drop table

H = Drop height for the table

V = Volume of the oil

B = Bulk modulus of the oil

t = Time

It follows from equation (2.2.1) that the magnitude of the pulse duration can be lowered by reducing the volume of the oil in the intensifier. The mass of the drop table should also be kept at minimum to obtain a lower value of the pulse duration. The upper limit of the duration of the loading cycle is limited by the amount of oil that can be filled in the intensifier, and the mass of the drop table which can be used without reducing the drop height to less than 2.5 inches.

For reducing the pulse duration, a new spacer was designed to reduce the volume of the oil in the oil chamber of the intensifier to approximately 3 cubic inches. A sectional view of the hydraulic intensifier with the new spacer is illustrated in Figure 14. The spacer also increases the elasticity of the system by preventing the cylindrical wall of the intensifier from being a part of the oil chamber. The analysis given in Appendix I shows that if the expansion of the cylindrical wall is prevented, the elasticity of the system results in a pulse duration of approximately 5 milliseconds. If the effect of the expansion of the wall is included, the

value of the pulse duration will be about 8 milliseconds. The magnitude of the pulse duration could not be increased beyond 90 milliseconds. This value was obtained by using a drop table weighing 250 lbs. A larger value for the mass of the drop table will make it necessary to drop the table from a height of less than 2.5 inches.

For measuring the pressure of the oil in the intensifier, it was decided to use a pressure transducer. A BLH(Baldwin-Lima-Hamilton) bonded strain gage pressure transducer was selected for this purpose. The transducer was connected to the lower portion of the intensifier as illustrated in Figure 4. Figure 14 of the intensifier shows the space provided for connecting the pressure transducer. The pressure pulse obtained from the transducer is shown in Figure 6. The upper trace in the figure, which was obtained from the load cell, is quite different from the lower trace obtained from the pressure transducer. Since the pressure transducer and the load cell monitor the input and output stress-time functions for the test specimen, it was expected that the two traces would have similar shapes.

To check the possibility that the odd shape of the pulse obtained from the pressure transducer might be due to the geometry of the path which connects the transducer with the main region of the oil chamber, the pressure transducer was connected to the upper part of the hydraulic intensifier. Figure 5 shows the pressure transducer connected to the oil

chamber through the air vent. The lower trace in Figure 7 shows the pressure pulse obtained with this configuration. The two pressure pulses shown in Figures 6 and 7 were obtained for exactly same values of the test variables ( the mass of the drop table, the drop height, the volume of the oil in the intensifier and the bias pressure etc.). The slight difference in the shapes of the two pulses verifies that the response of the pressure transducer is also a function of the geometry of the path which connects the transducer with the oil chamber.

The failure of the pressure transducer to respond to the pressure variations at the end of the main pulse, further confirms that the load cell gives a much better response to the pressure in the oil chamber. These pressure variations are caused as a result of the collision of circlip ( connected to the drive piston) with the chamber. Figures 6 and 7 very clearly show that the load cell is very sensitive to these pressure variations.

The inability of the pressure transducer to accurately record the pressure in the hydraulic intensifier, ultimately led to the pressure pulse being monitored by a strain gage cemented to the cylindrical wall of the intensifier. Figure 2 illustrates the strain gage bonded to the wall of the oil chamber. An analysis for the response of the strain gage to the pressure of the oil in the chamber is given in Appendix I. The shape of the pressure pulse obtained from the strain gage compared

well with the load pulse obtained from the load cell. The lower traces in Figures 8 to 13 have been obtained from the strain gage.

### 2.3 Test Procedure

The experiments were performed on mild steel samples. Two mild steel rods were used for the preparation of the test samples. The rods were analysed as:

Rod A	Carbon	0.39 %	Sulphur	0.052 %
Rod B	Carbon	0.44 %	Sulphur	0.055 %

The test samples were made according to the dimensions prescribed for the cylindrical medium length ASTM compression test specimen.

Length: 1.5 "  $\pm$  0.05 "

Diameter: 0.5 "  $\pm$  0.01 "

The test samples of both batches were annealed by maintaining the temperature at 900°C for one hour, and then gradually cooled while still in the oven.

Each sample was assigned an identification number. The first digit represented the batch, the second, the duration of the loading, and the last, the serial number of the sample in the tests performed for a particular pulse duration. If more than nine samples were tested for the same duration of the loading, the last two digits represented the serial number.

The dimensions of the samples, before and after loading, were measured with the aid of a Starret Dial Indicator (No. 656-617) having an accuracy of 0.0001 inch, and a range of 0.4 inch. The range was increased by using the gage blocks.

A dual beam Tektronix oscilloscope, Type 565, and two carrier amplifiers, Type 3C66, were used to obtain the load and the pressure pulses from the load cell and the strain gage, which were connected to the two carrier amplifiers. As the carrier amplifier also supplied the excitation voltage for the transducers, no external voltage source was required. The coordinates of the oscilloscope traces, recorded on Polroid film, were subsequently measured with the aid of a Wilder Micro Projector (Figure 3). The oscilloscope traces were photographed using a, Type C-27, Tektronix camera.

The use of the new spacer prevents the air vent from removing the air from the oil chamber. To ensure that the intensifier was free from air, the spacer was filled to the top with the oil, and then the drive piston inserted. The

spacer also prevents the use of circlip on the drive piston. As the O-ring between the spacer and the drive piston can not withstand a pressure of more than 20 psi, a higher bias pressure could not be used. The introduction of the spacer also prevents the strain gage from recording the pressure pulse.

More details about the test procedure are given in References 1 and 2.

#### 2.4 Test Results

A few typical oscilloscope traces illustrating stress-time functions for different values of the plastic strain are shown in Figures 8 to 13. Each photograph shows two sets of superimposed stress pulses. The upper set has been obtained from the load cell and the lower set corresponds to the response of the strain gage. The two stress pulses in each set correspond to the tests on the fully hardened and the mild steel samples. The difference between the two pulses increases with increase in the plastic strain in the test sample. The stress-time function for the fully hardened sample approximates a half sine curve. For higher values of the plastic strain, the stress pulse shows a sharp upper yield point. The stress corresponding to the yield point has been defined as

yield stress. For the stress pulses, which do not exhibit a sharp yield point, the yield stress has been represented by the maximum stress achieved during the loading. For very large plastic strain, the stress-time function exhibits two maxima, and in some cases the value of the yield stress is less than the stress corresponding to the other peak point. For all such cases, the calculation of the form function has been done on the basis of the yield stress.

The peak load for the elastic test is plotted against the drop height as illustrated in Figure 17. The values of the peak load were obtained from the load-time functions for the fully hardened sample. As expected the logarithmic plot between the two variables exhibits a linear relationship. The coefficients of the straight lines for different pulse durations were obtained by the method of least squares.

The values of the yield stress, the nominal peak stress, and the permanent strain for each test are listed in Tables 5 and 7. The nominal peak stress is the value of the peak stress which would have been obtained if the test sample had remained elastic throughout the entire loading cycle. The values of the nominal peak load were obtained with the aid of Figure 17. Figure 18 illustrates the plot of the residual strain against the nominal peak stress for the samples of Batch A. In the region for which the value of the residual strain is less than two percent, the plot exhibits a linear relationship between

the two variables. The coefficients for the straight lines corresponding to different pulse durations were again obtained by the least squares method. The value of 'Apparent Dynamic Yield Stress' corresponding to each pulse duration can be determined by finding the intercept of the least squares line with the zero residual strain coordinate.

Table 7 gives the values of the yield stress, the nominal peak stress, and the permanent strain for the test samples of batch B. Figure 19 exhibits the plot of the nominal peak stress versus the residual strain. With the exception of the 18 milliseconds pulse duration, no proper correlation could be found between the two variables for any pulse duration.

The value of the flow function for zero plastic strain can be determined by substituting the value of the pulse duration and the corresponding value of the apparent dynamic yield stress in equation (1.6). The value of the material constant 'n' can then be determined by equating any two values of the flow function. The values of 'n' determined in this manner are listed in Table 8. Figure 20 exhibits a log-log plot of the apparent dynamic yield stress and the pulse duration. The value of 'n' obtained from the slope of the least squares line for this plot is listed in Table 9. As no proper correlation could be found between the nominal peak stress and the residual strain for batch B, the values of the apparent dynamic yield stresses could not be determined.

Figures 21 and 22 illustrate the values of the peak stress obtained from the stress pulses for the mild steel samples plotted against the residual strain in the test sample. The figures indicate that the material of batch A is slightly more responsive to the dynamic loading.

Tables 10 and 11 give the values of the yield stress and the time elapsed to reach the yield point. The values are listed for only those test samples, which exhibited a sharp upper yield point in the stress-time function. The value of the material constant 'n' has been determined by equating the values of the flow function corresponding to the plastic strain at the yield point. The samples with approximately equal form functions have been grouped, and the value of 'n' has been determined on the basis of the slope obtained for the least squares line for a log-log plot between the yield stress and the time required to reach the yield point. The values of 'n' are also listed in Tables 10 and 11.

For the test samples which exhibited a sharp yield point, the values of the yield stress have been plotted against the rate of strain. The value of the strain rate was determined by assuming that below the yield point, the stress varies linearly with time. Figures 23 and 24 illustrate the log-log plots between the two variables. The value of the slope for the least squares line was used to determine the value of the material constant

'n'. The data and the values of 'n' are listed in Tables 12 and 13.

Figures 25 and 26 illustrate the plots of the flow function against the residual strain. The data is listed in Tables 14 and 15. The figures also show the theoretically derived curves obtained from reference 1. The curves which were originally determined for a value of 23.5 for the material parameter 'n', have been slightly modified for the values of 'n' obtained for mild steel.

A plot of the apparent peak load against the mass of the drop table is illustrated in Figure 27. The values of the apparent peak load correspond to the drop height of 10 inches, and were obtained with the aid of Figure 17. Figure 28 exhibits the plot between the mass of the drop table and the corresponding value of the pulse duration.

Figures 29,30,32 and 33 present plots of the residual strain against the energy required to produce the plastic strain. Figures 29 and 30 illustrate the values of energy evaluated by multiplying the weight of the drop table with the difference in the heights of the rebound corresponding to the tests on fully hardened and mild steel samples. This method gives a very rough estimate of the energy dissipated in yielding. The value of the yield stress determined on the basis of these

results is found to be about 62 kpsi for both batches. The stress pulses for the test samples indicate that the average value for the yield stress should be about 70 kpsi. Figures 32 and 33 show the values of energy determined on the basis of the nominal peak stress and the mid-point value of the stress for the test sample. The details of this method are given in Appendix III. The value of spring constant used for this method has been determined by assuming that the average value of the yield stress is 70 kpsi. Therefore, this technique can not give very accurate values for energy, but can predict the nature of the plots relating the residual strain and the energy dissipated in yielding.

The details about the techniques used to obtain the results are described in Appendix II.

## CHAPTER 3

### DISCUSSION AND CONCLUSIONS

#### 3.1 Dynamic Response of Mild Steel

The test specimens made from two mild steel rods having different percentage of carbon were tested under dynamic loading. The steel containing less carbon exhibited slightly greater strain rate response. This is indicated by Figures 21 and 22, which illustrate the plots of the peak stress against the residual strain for different durations of loading. The figures show that for a particular value of the residual strain, the variation in the values of the peak stress with loading duration is slightly more in the case of the test samples of Batch A. A lower value of the material parameter 'n' obtained for the steel having lower percentage of carbon also supports this view. The limited range of the duration of loading, and the scatter in the results prevent the plots (Figures 21 and 22) from exhibiting any significant relationship between the variables.

The comparison of the results with the static tests shows an increase of about 40 percent in the yield stress of the material.

### 3.2 Correlation with Theory

The values of 'Apparent Dynamic Yield Stress' obtained for batch A show good correlation with design equation (1.6). The least squares lines obtained for the log-log plot between apparent dynamic yield stress and the duration of loading exhibit a correlation coefficient of .99, and thus, indicate the validity of equation (1.6). The values of material constant 'n' obtained by using equation (1.11) compare well with the results obtained with the application of equation (1.6). The values of material parameter 'n' are in agreement with the results obtained by other researchers. The values of 'n' are listed in Table 1.

The nature of the plots between the flow function and the residual strain correspond with the theoretical curves obtained from Reference 1.

### 3.3 Correlation Between Nominal Peak Stress and Residual Strain

The analysis done for ideally elastic-plastic material in Appendix III shows that a linear relationship can be expected between the nominal peak stress and the residual strain. This is indicated by the theoretical curves shown in Figure 31. For large plastic strain, the effects of strain hardening and the increase in the diameter of the test sample become significant. As a result, for higher values of the residual strain, the nature of the plots (Figures 19 and 20) based on experimental results

differs from the theoretically derived curves.

The analysis shows that the slope of the plot between the residual strain and the nominal peak stress is basically a function of the spring constant for the hydraulic intensifier. The same conclusion can be drawn on the basis of the experimental results. The plots for pulse durations of 32, 40, 62 and 90 milliseconds in Figures 19 and 20 do not show any appreciable difference. The tests for these pulse durations were done with the same amount of oil in the intensifier.

The superimposed theoretical curves in Figures 19 and 20 exhibit good correlation with the experimental results.

### 3.4 Flexibility of the Tester

The use of spacers in the hydraulic intensifier prevents the pressure from being uniform in the oil chamber. This is indicated by the load-time traces, which show that during loading the pressure in the intensifier does not rise smoothly. The problem can be overcome by using a drive piston of larger diameter for reducing the pulse duration. The use of a drive piston of larger diameter will also increase the elasticity of the system, and thus, will further reduce the duration of the loading. The upper limit of the duration of the loading can be similarly raised by reducing the diameter of the drive piston.

### 3.5 Monitoring the Pressure Pulse

A strain gage cemented on the wall of the hydraulic intensifier was used to record the pressure of the oil. The pressure pulse which exhibits the force-time function, input to the test sample, was observed to be exactly same as the load pulse obtained from the load cell. Figures 8 to 13 exhibit the oscilloscope traces obtained from the load cell and the strain gage.

### 3.6 Recommendations for Future Work

- (i) Additional drive pistons of different diameters should be used to increase the range of the pulse durations.
- (ii) The method for determining the height of rebound of the drop table should be modified. This will help in giving a better estimate of the energy dissipated in the yielding of the test sample.
- (iii) A technique should be developed to record the stroke of the drive piston.
- (iv) The experiments should be performed to study the effect of multiple impulses with varying intervals of time between the loadings.

## APPENDIX I

### ANALYSIS OF THE SYSTEM

#### I.1 Elasticity of the System

The effect of the elasticity of the system on the duration of the loading pulse can be studied by evaluating the increase in the volume of the oil chamber, when the oil is subjected to pressure. The main factors which contribute to the expansion of the oil chamber, are as follows:

(i) Increase in the diameter of the cylindrical wall of the intensifier

The increase in the internal radius of the wall evaluated using Lamé equations is given by the following expression:

$$\Delta r = 14.5P / E$$

The increase in the radius effects an increase in the volume of the oil chamber, which can be expressed as:

$$\Delta V = 1183P / E$$

The displacement of the drive piston caused by the

increase in the volume of the oil chamber is as follows:

$$x = 1340 P / E$$

(ii) Increase in the length of the six bolts

The pressure in the intensifier effects an increase in the tensile stress in the bolts. The increase in the length of each bolt due to the tension can be expressed as:

$$\Delta L = 318 P / E$$

The resultant increase in the volume of the oil chamber is given by:

$$\Delta V = 725 P / E$$

This results in a displacement of the drive piston, which can be expressed as:

$$x = 822 P / E$$

(iii) Compression of the test sample

The displacement of the drive piston, caused due to the compression of a standard test sample ( 1.5" long and 0.5" diameter ) is given by:

$$x = 600 P / E$$

(iv) Compression of the drive piston

The displacement of the drive piston caused by this factor is the compression of the drive piston itself. It can be expressed as:

$$x = 9.5 P / E$$

The total displacement of the drive piston caused by these four factors is as follows:

$$x = 2772 P / E$$

The equivalent spring constant will be:

$$W = P A_3 / E$$

$$= E / 3120$$

where  $A_3 =$  Area of the drive piston

For a drop table weighing 24 lbs ( minimum weight for the drop table ) the pulse duration is given by

$$t_E = \pi / \sqrt{W/M}$$

$$= 8.04 \text{ milliseconds}$$

This value of the pulse duration is caused due to the elasticity of the system, and could be obtained experiment-

ally if the bulk modulus of the oil filled in the intensifier were infinite.

The use of the new spacer prevents the cylindrical wall from being a part of the oil chamber, and therefore, the expansion of the wall does not contribute to the increase in the volume of the chamber. The area which transfers the force to the bolts is also reduced. The displacement of the drive piston due to this factor in the new configuration is approximately given by

$$x = 550 P / E$$

This configuration effects an increase in the elasticity of the system, and the resultant value of the pulse duration will be:

$$t_E = 5.26 \text{ milliseconds}$$

The duration of loading obtained while using this spacer was 13 milliseconds. For an infinite value of the elasticity of the system, the following value of the pulse duration would have been obtained.

$$\begin{aligned} t_\infty &= \sqrt{t_0^2 - t_E^2} \\ &= \sqrt{13^2 - (5.26)^2} \\ &= 11.9 \text{ milliseconds} \end{aligned}$$

## I.2 Response of the Strain Gage

In ordinary condition, when the oil in the intensifier is at normal pressure, the cylindrical wall of the intensifier is subjected to a compressive force due to the tightening of the bolts. During the loading, the bolts are subjected to a further tensile stress, which causes the elongation of the bolts, and thus, results in the release of the compressive force in the cylindrical wall. The strain gage, therefore, records a lower value of the strain than what it should do at a particular pressure. The strain gage is subjected to approximately  $20 \times 10^{-6}$  strain. The corresponding compressive stress in the wall is completely released at a pressure of about 1200 psi.

The ratio of the strain exhibited by the load cell to the strain recorded by the strain gage (after being corrected for the above error) has been found to be 3.98. This value agrees with the result determined analytically.

## APPENDIX II

### EVALUATION OF THE RESULTS

#### II.1 Determination of Stress-Time Function

The load-time trace for each sample was produced on a transparent slide, and the coordinates of the function were measured with the aid of a Wilder Micro Projector (Figure 3). For determining the form function by numerical integration, the base of the function was divided into twenty intervals and the value of the stress was determined for nineteen points. Though, for calculating the form function for the whole pulse, it would have been sufficient to determine only those stresses which were more than 75 percent of the peak value, the evaluation of the flow function corresponding to the plastic strain at the yield point made it necessary to calculate the values of the lower stresses as well. The value of the peak load for the load pulse for the elastic test was also determined for each test.

The amplifier used in the oscilloscope records the load in terms of strain. For measuring the signal produced by the load cell, the following analysis is required.

Let the resistance of each of the four arms of the wheatstone bridge be R, the output is then given by the following expression:

$$\Delta V/V = \Delta R/4R \quad \text{--(II.1.1)}$$

The value of the change in resistance,  $\Delta R$ , can be expressed as:

$$\Delta R/R = (\text{Gage Factor}) \times (\text{Strain}) \quad \text{--(II.1.2)}$$

The above two relations can be used to obtain the following expression:

$$\Delta V/V = (\text{G.F.} \times \text{Strain})/4 \quad \text{--(II.1.3)}$$

As the 3C66 amplifier is calibrated for a gage factor of 2, it follows that the oscilloscope will record one  $\mu$ strain for an output of  $5 \times 10^{-7}$  Volt/Volt. Since the output of the load cell at full capacity (50,000 lbs) is 2mV/Volt, the oscilloscope will exhibit 4000  $\mu$ strain for a load of 50,000 lbs.

## II.2 Determination of 'n'

The material parameter 'n' is the most important factor for predicting the behaviour of the material under any loading cycle. For small plastic strain, the value of the flow function depends only on the residual strain. The value of 'n', therefore, can be determined by equating flow functions for two samples which have been subjected to same plastic strain. Also, for small value of the residual strain, the form of the stress pulse is similar to a half sine curve, and therefore, the values of the form function for the two stress functions

may be assumed equal. The example given below illustrates the use of this method to determine the value of 'n'.

Sample No.	Duration of Loading (ms)	Peak Stress (kpsi)	Residual Strain (percent)
117	13.01	74.95	0.06
162	62.43	70.12	0.07

Using equation (1.6) the values of the flow functions can be expressed as:

$$(74.95)^n \times 13.01 \times K(n) = H(0.06)$$

$$\text{and } (70.12)^n \times 62.43 \times K(n) = H(0.07)$$

Assuming  $H(0.06)$  to be approximately equal to  $H(0.07)$ , and neglecting any difference in the form functions, the following relation may be obtained.

$$(74.95)^n \times 13.01 = (70.12)^n \times 62.43$$

On simplification, the above equation yields

$$n = 23.9$$

The method discussed above uses the results of only two test samples, and since there is a large scatter in the results, the value of 'n' obtained by this method can not be very reliable.

The values of 'n' determined by equating the values of the flow function for zero plastic strain are listed in Table 8. This procedure uses the values of the apparent dynamic yield stress, which is an extrapolated value of the peak stress for zero residual strain. Therefore, the value of 'n' obtained using this method depends on the results of a large number of test samples.

The value of 'n' listed in Table 9 has been determined by plotting the log of apparent dynamic yield stress against the log of loading duration. Taking the log of both sides of equation (1.6), the following expression is obtained:

$$n \log(\sigma_m) + \log(t_0) + \log(K(n)) = \log(H(\epsilon)) \quad \text{--(II.2.1)}$$

For zero plastic strain, the values of  $\log(K(n))$  and  $\log(H(\epsilon))$  would be independent of the value of the loading duration. Therefore, the log-log plot between apparent dynamic yield stress and duration of loading would exhibit a linear relationship. The slope of the least squares line has been used to evaluate the value of 'n'. Since this method uses the results of very large number of test samples, the value of 'n' obtained by this technique is expected to be quite accurate.

The value of 'n' can also be determined by equating the flow functions corresponding to the plastic strain at the yield point. Taking two test samples, which exhibit a sharp

yield point, an approximate value of the constant 'n' can be determined by assuming that the values of the form functions corresponding to the yield points for the two cases are equal. This value of 'n' can now be used to evaluate the flow functions by numerical integration. The values of the flow functions and 'n' can be used to obtain a better value of the parameter 'n'. This iterative procedure may be used to determine the value of 'n' which would give equal values of the flow function for the two cases.

Assuming  $\sigma_y(1)$  and  $\sigma_y(2)$  as the values of the yield stress, and  $t_y(1)$  and  $t_y(2)$ , the values of time elapsed before reaching the yield point, an approximate value of 'n' can be determined by using the following expression:

$$n = \log(t_y(1)/t_y(2))/\log(\sigma_y(2)/\sigma_y(1)) \quad \text{--(II.2.2)}$$

If  $H_1(\epsilon_y)$  and  $H_2(\epsilon_y)$  be the values of the flow function obtained by numerical integration using this approximate value of 'n', an improved value of 'n' can be obtained by using the following relation:

$$n = n + \log(H_1(\epsilon_y)/H_2(\epsilon_y))/\log(\sigma_y(2)/\sigma_y(1)) \quad \text{--(II.2.3)}$$

where  $\epsilon_y$  = Plastic strain at the yield point

The example given below illustrates the use of this method.

Sample No.	Yield Stress (kpsi)	Time Elapsed Before Reaching Yield Point (ms)
118	78.08	5.94
143	74.46	19.65

Substitution of these values in equation (II.2.2) yields:

$$n = 25.13$$

The following table gives the subsequent values of 'n' obtained after each iteration.

S.No.	n	$H_1(\epsilon_y)$	$H_2(\epsilon_y)$
1	25.13	$3.14 \times 10^{47}$	$2.87 \times 10^{47}$
2	23.26	$9.27 \times 10^{43}$	$9.19 \times 10^{43}$
3	23.09	$4.47 \times 10^{43}$	$4.46 \times 10^{43}$

Hence,  $n = 23.09$

Again, since the value of 'n' obtained by this method depends only on two individual tests, the reliability of the result cannot be assessed.

A better value of 'n' can be obtained by selecting the test samples for which the form functions corresponding

to the yield point are approximately equal. This can be done by calculating the ratio of the yield stress to the nominal peak stress for each test sample which exhibits a sharp yield point, and then grouping those samples for which this ratio is approximately same. The value of 'n' can now be obtained with the aid of a log-log plot between yield stress and the time elapsed before yielding. The values of 'n' determined by using this technique are listed in Tables 10 and 11.

The value of the material parameter 'n' can also be evaluated by using a log-log plot of yield stress versus strain rate. The following expression is obtained by taking the log of both sides of equation (1.11).

$$\log (\sigma_y) = (1/(n+1)) \log (\dot{\epsilon}) + \log (C_3) \quad \text{--(II.2.4)}$$

It follows from the above equation that the slope of the least squares line for the log-log plot would be equal to  $1/(n+1)$ . For each test sample, which exhibits a sharp yield point in the stress time trace, an approximate value of the strain rate can be determined by assuming that below the yield point, the stress increases linearly with time. As this method uses the results of a large number of samples, the value of 'n' is expected to be quite accurate. The results obtained by this technique are listed in Tables 12 and 13.

For determining flow functions, the following values of 'n' have been used for the two batches.

<u>Batch</u>	<u>n</u>
A	23
B	33

### II.3 Evaluation of Flow Function

Since the stress-time pulse for the test sample does not follow any particular function, the value of the flow function for each test sample was determined by numerical integration. For each stress-time function, the values of the stresses were determined at nineteen points. The values of the ordinates for evaluating the flow function were obtained by raising the values of the stresses to the power 'n'. The value of the flow function was then determined using Simpson's rule. A detailed description of the procedure is given in Reference 2.

### II.4 Estimation of the Energy Dissipated in Yielding

An approximate value of the energy required to produce plastic strain in the test sample can be determined by calculating the difference in the heights of rebound for the mild steel and fully hardened samples. The product of the weight of the

drop table and the difference in the heights for the two tests gives an estimate of the energy dissipated in the yielding of the test sample.

The value of the energy has also been estimated on the basis of stress pulses for the two tests. The details of this technique are described in Appendix III.

## APPENDIX III

### ANALYSIS FOR DETERMINING RELATION BETWEEN NOMINAL PEAK STRESS AND RESIDUAL STRAIN

The difference in the stress-time functions for the tests on fully hardened and mild steel samples increases with the increase in the plastic strain in the test sample. Since the drop table is allowed to fall from the same height for the two tests, an equal amount of energy is fed in the system for both cases. The energy, which can be recovered from the system depends on the value of the stress at the instant, when the drive piston starts moving back (assuming that no plastic strain takes place after that instant). The difference between the values of recoverable energy for the two cases should give an estimate of the amount of energy required to produce the plastic strain in the test sample.

Assuming that the specimen is made of an ideally elastic-plastic material, the stress-time pulse will have the form as illustrated in Figure 16. The difference in the values of the recoverable energy for the two tests may be expressed as:

$$(W/2) (x_e^2 - x_y^2) \quad \text{--(III.1)}$$

where  $W$  is the spring constant for the drive piston and,  $x_e$  and  $x_y$ , the displacements of the drive piston required to produce the stresses  $\sigma_e$  and  $\sigma_y$  respectively. The displacements of the drive piston may be expressed as:

$$x_e = ( \sigma_e A_1 A_3 ) / ( A_2 W )$$

$$x_y = ( \sigma_y A_1 A_3 ) / ( A_2 W ) \quad \text{--(III.2)}$$

Substitution of these values in expression (III.1) yields:

$$( A_1 A_3 / A_2 )^2 ( \sigma_e^2 - \sigma_y^2 ) / 2 W \quad \text{--(III.3)}$$

An expression relating residual strain and the energy required to produce the residual strain can be obtained on the basis of an estimated value for the yield stress. The test results for mild steel show that 70 psi will be a reasonable value for the yield stress. The energy required to produce residual strain,  $\epsilon_r$ , may be expressed as:

$$\sigma_y A_1 L_1 \epsilon_r \quad \text{--(III.4)}$$

where  $L_1$  is the length of the test sample.

Since the test apparatus does not have any means for measuring the displacement of the drive piston, it is not possible to determine the exact value of  $W$ , the spring constant for the drive piston. The system also does not behave exactly as a lumped mass system, and therefore, it is not possible to obtain the value of  $W$  on the basis of the values of the mass of the drop table and the pulse duration.

Expression (III.3) can be used to determine the value of energy required to produce plastic strain in each test sample. The value of the stress at the instant, when the drive piston starts moving back, may be substituted for  $\sigma_y$ . The value of this stress is approximately given by the mid-point value of the stress for the stress-time trace obtained for the test sample. An approximate value of  $W$ , the spring constant, may be obtained by comparing the values of energy determined using expressions (III.3) and (III.4).

Using the method discussed above, the following values of  $W$  have been obtained for different durations of loading:

Pulse Durations (milliseconds)	Spring Constant (lbs/inch)
32, 40, 62 and 90	1000
13 and 17	4000

These values of the spring constant may now be used in expression (III.3) to estimate the energy required to produce plastic strain in each test sample. These values have been plotted in Figures 32 and 33.

On substituting the numerical values in expressions (III.3) and (III.4) and equating them, the following relation is obtained:

$$218 ( \sigma_e^2 - \sigma_y^2 ) / W = .0294 \sigma_y \epsilon_r \quad \text{---(III.5)}$$

where  $\sigma_e$  and  $\sigma_y$  are in kpsi,  $\epsilon_r$  in percent, and  $W$  in lbs per inch.

The expression (III.5) may be rewritten in the following form:

$$\sigma_e / \sigma_y = ( 1 + .0294 \epsilon_r W / 218 \sigma_y )^{1/2} \quad \text{---(III.6)}$$

Substitution of 70 kpsi for  $\sigma_y$  in the right hand side of the above expression yields:

$$\sigma_e / \sigma_y = \sqrt{ ( 1 + .000193 W \epsilon_r ) } \quad \text{---(III.7)}$$

The curves illustrated in Figure 31 have been obtained with the aid of equation(III.7). The curves for the two values

of the spring constant indicate that for lower values of the plastic strain ( less than two percent ), nominal peak stress and residual strain should exhibit a linear relationship.

APPENDIX IV

TABLES

TABLE 1

ROOM TEMPERATURE VALUE OF MATERIAL PARAMETER 'n'  
FOR VARIOUS IRON ALLOYS

<u>MATERIAL</u>	<u>'n'</u>	<u>SOURCE</u>	<u>REFERENCE</u>
Mild Steel	14	Krafft	(4)
SAE 4340 Rc 30	20	Kardos	(1)
Fe	21	Hull & Noble	(6)
Mild Steel	22	Winlock	(4)
Mild Steel	23	Fisher & Rogers	(4)
Mild Steel	25	Clark & Wood	(7)
Mild Steel	33	Winlock	(4)
Mild Steel	34	Sylwestrowicz & Hall	(4)
Fe-3.25% Si Crystals	35	Stein & Low	(4)
Mild Steel (0.39% C)	23	This Thesis	
Mild Steel (0.44% C)	33	This Thesis	

TABLE 2VARIATION OF PULSE DURATION WITH TEST APPARATUS PARAMETERS

<u>WEIGHT OF THE</u> <u>DROP TABLE</u> (lbs)	<u>VOLUME OF THE OIL IN</u> <u>THE INTENSIFIER</u> (cubic inches)	<u>DURATION OF</u> <u>LOADING</u> (ms)
24	3	13
36	4	17
86	120	32
59	120	40
138	120	62
250	120	90

TABLE 3STATIC TEST RESULTS

<u>SAMPLE NO.</u>	<u>STRESS</u> (kpsi)	<u>PERMANENT STRAIN</u> (percent)
101	54.20	1.40
	65.00	2.69
	75.90	3.95
102	50.00	0.13
	51.00	0.46
	59.05	1.82
201	50.00	0.05
	52.00	0.87
	52.40	1.35
	59.05	1.89
202	68.8	2.78
203	52.5	0.01

TABLE 4

## BATCH A

SAMPLE NO.	DROP HEIGHT (INCHES)	PEAK LOAD(LBS) (OBTAINED FROM ELASTIC TEST)
111	9.50	10438
112	12.50	11364
113	15.50	12779
114	18.50	14168
115	22.50	15666
116	24.50	16710
117	20.50	14889
118	22.50	15892

PULSE DURATION = 13.0 MS

121	11.00	13991
122	12.75	15345
123	15.80	16914
124	20.00	19787
125	24.00	21771

PULSE DURATION = 17.0 MS

131	38.70	14367
132	48.70	16032
133	36.50	14311
134	33.50	13509
135	28.50	12483
136	43.50	15552
137	53.50	17678

PULSE DURATION = 32.0 MS

141	17.70	12677
142	20.20	13682
143	22.70	14523
144	27.70	16375
145	32.60	18126
146	37.60	19562
147	18.56	13153
148	19.06	13419

PULSE DURATION = 40.0 MS

TABLE 4 (CONTD.)

SAMPLE NO.	DROP HEIGHT (INCHES)	PEAK LOAD(LBS) (OBTAINED FROM ELASTIC TEST)
151	3.10	13431
152	3.60	14263
153	2.85	13023
154	3.35	13957
155	4.10	15227
156	5.10	17101
157	2.37	11973
158	2.62	12639
159	6.25	18855

PULSE DURATION = 90.0 MS

161	6.25	12920
162	6.75	13282
163	7.25	13833
164	8.25	14887
165	9.25	15632
166	10.75	16846
167	12.75	18578
168	7.00	13480
169	7.75	14225
1610	7.00	13491

PULSE DURATION = 62.0 MS

TABLE 5

## BATCH A

SAMPLE NO.	YIELD STRESS (KPSI)	NOMINAL PEAK STRESS (KPSI)	PERMANENT STRAIN (PERCENT)
111	50.56	50.40	.02
112	58.98	58.82	.03
113	66.19	66.30	.03
114	71.57	73.11	.02
115	77.41	81.80	.49
116	81.40	85.63	.42
117	74.95	77.49	.06
118	78.08	81.41	.32

PULSE DURATION = 13.0 MS

121	71.42	72.36	.01
122	76.30	78.54	.11
123	81.28	88.59	.71
124	80.78	101.34	1.38
125	86.54	111.93	1.91

PULSE DURATION = 17.0 MS

131	73.48	76.37	.59
132	74.82	86.01	2.19
133	73.46	74.57	.56
134	70.13	71.35	.25
135	65.82	65.50	.02
136	77.26	81.53	1.86
137	81.89	90.76	2.46

PULSE DURATION = 32.0 MS

141	66.92	67.20	.02
142	71.61	72.29	.10
143	74.46	77.15	.98
144	75.80	86.22	2.23
145	80.49	94.17	2.62
146	80.22	102.05	3.00
147	69.52	69.15	.03
148	70.08	70.09	.13

PULSE DURATION = 40.0 MS

TABLE 5 (CONTD.)

SAMPLE NO.	YIELD STRESS (KPSI)	NOMINAL PEAK STRESS (KPSI)	PERMANENT STRAIN (PERCENT)
151	70.51	71.13	.09
152	76.87	79.43	1.42
153	67.99	68.63	.14
154	70.76	73.64	1.15
155	74.94	81.02	1.87
156	75.60	89.01	2.36
157	63.39	63.12	.03
158	66.83	66.05	.03
159	73.51	97.89	3.10

PULSE DURATION = 90.0 MS

161	67.38	67.48	.02
162	70.12	70.25	.07
163	72.02	72.82	.61
164	75.24	77.68	1.31
165	76.19	82.18	1.83
166	76.15	88.91	2.29
167	79.67	96.80	2.76
168	69.45	71.69	.70
169	73.41	75.30	.82
1610	70.46	71.58	.07

PULSE DURATION = 62.0 MS

TABLE 6

## BATCH B

SAMPLE NO.	DROP HEIGHT (INCHES)	PEAK LOAD(LBS) (OBTAINED FROM ELASTIC TEST)
211	17.50	12795
212	19.50	13835
213	20.50	13853
214	21.50	14227
215	23.50	15246

PULSE DURATION = 13.5 MS

221	15.00	15275
222	13.00	14419
223	18.00	17893
224	22.00	19340
225	25.00	20633

PULSE DURATION = 18.0 MS

231	28.50	12337
232	33.50	13581
233	38.50	14531
234	48.50	16430
235	53.50	17474

PULSE DURATION = 32.0 MS

241	17.60	12893
242	20.10	13884
243	22.60	14929
244	27.60	16612
245	32.60	17890
246	18.81	13293

PULSE DURATION = 40.0 MS

TABLE 6 (CONTD.)

SAMPLE NO.	DROP HEIGHT (INCHES)	PEAK LOAD(LBS) (OBTAINED FROM ELASTIC TEST)
251	2.50	12297
252	2.75	12874
253	3.00	13380
254	2.75	12815
255	3.25	13899
256	4.25	16072
257	5.25	17304
258	6.25	18652

PULSE DURATION = 90.0 MS

261	6.75	13274
262	6.50	13089
263	7.00	13577
264	7.25	13819
265	8.25	14738
266	10.25	16600
267	13.25	18985

PULSE DURATION = 62.0 MS

TABLE 7

BATCH B

SAMPLE NO.	YIELD STRESS (KPSI)	NOMINAL PEAK STRESS (KPSI)	PERMANENT STRAIN (PERCENT)
211	66.46	66.65	.03
212	66.52	70.75	.13
213	68.95	72.87	.07
214	69.49	74.85	.39
215	75.50	78.77	.46

PULSE DURATION = 13.5 MS

221	75.31	80.66	.45
222	72.15	74.57	.14
223	74.35	89.66	.86
224	78.84	100.31	1.43
225	81.47	107.72	1.77

PULSE DURATION = 18.0 MS

231	65.18	65.35	.01
232	68.41	71.27	.40
233	75.27	76.85	1.02
234	78.65	86.69	2.20
235	77.53	91.56	2.30

PULSE DURATION = 32.0 MS

241	67.37	68.38	.01
242	72.62	73.30	.23
243	74.65	77.71	1.19
244	75.09	86.50	2.18
245	76.03	94.65	2.62
246	69.24	70.84	.34

PULSE DURATION = 40.0 MS

TABLE 7 (CONTD.)

SAMPLE NO.	YIELD STRESS (KPSI)	NOMINAL PEAK STRESS (KPSI)	PERMANENT STRAIN (PERCENT)
251	65.00	65.24	.02
252	66.05	68.28	.43
253	69.69	70.92	.33
254	67.08	68.31	.03
255	71.06	73.64	1.00
256	71.07	83.16	2.13
257	73.78	91.39	2.45
258	75.69	99.03	2.94

PULSE DURATION = 90.0 MS

261	69.14	70.69	.41
262	68.32	69.31	.03
263	69.91	71.96	.67
264	71.92	73.29	.45
265	72.02	78.23	1.46
266	74.85	87.55	2.19
267	77.66	99.87	2.92

PULSE DURATION = 62.0 MS

TABLE 8

BATCH A

<u>APPARENT DYNAMIC</u> <u>YIELD STRESS</u> $\sigma_y(1)$ (kpsi)	<u>DURATION OF</u> <u>LOADING</u> $t_0(1)$ (ms)	<u>APPARENT DYNAMIC</u> <u>YIELD STRESS</u> $\sigma_y(2)$ (kpsi)	<u>DURATION OF</u> <u>LOADING</u> $t_0(2)$ (ms)	<u>MATERIAL</u> <u>PARAMETER</u> 'n'
73.77	13.0	67.75	90.0	<u>22.7</u>
73.77	13.0	68.95	62.0	<u>23.1</u>
73.77	13.0	69.81	40.0	<u>20.4</u>
72.72	17.0	69.81	40.0	<u>20.9</u>
72.72	17.0	67.75	90.0	<u>23.5</u>
72.72	17.0	68.95	62.0	<u>24.2</u>
68.95	62.0	67.75	90.0	<u>21.2</u>

TABLE 9

BATCH A

<u>APPARENT DYNAMIC YIELD STRESS</u> (kpsi)	<u>DURATION OF LOADING</u> (ms)
73.77	13.0
72.72	17.0
71.31	32.0
69.81	40.0
68.95	62.0
67.75	90.0

Value of material parameter 'n'

obtained from the log-log plot = 22.95

TABLE 10

BATCH A

VALUE OF THE MATERIAL PARAMETER 'n' OBTAINED ON THE BASIS  
OF LOG-LOG PLOT BETWEEN YIELD STRESS AND TIME TO YIELD

<u>SAMPLE NO.</u>	<u>LOADING TIME FOR PRODUCING</u> <u>YIELD (ms)</u>	<u>YIELD STRESS</u> <u>(kpsi)</u>
124	4.90	80.77
136	13.20	77.25
155	34.54	74.93
165	24.66	76.18
<u>Value of the material parameter 'n' = 26.18</u>		
115	5.71	77.41
116	5.76	81.40
118	5.94	78.08
123	6.89	81.28
143	19.65	74.46
152	40.43	76.77
154	38.32	70.75
164	27.52	75.23
<u>Value of the material parameter 'n' = 25.1</u>		
132	12.23	74.81
137	11.61	81.88
144	14.55	75.79
145	13.32	80.49
156	31.66	75.59
166	20.93	76.13
<u>Value of the material parameter 'n' = 21.7</u>		

TABLE 11

BATCH B

VALUE OF MATERIAL PARAMETER 'n' OBTAINED ON THE BASIS OF  
LOG-LOG PLOT BETWEEN YIELD STRESS AND TIME TO YIELD

<u>SAMPLE NO.</u>	<u>TIME TO YIELD</u> (ms)	<u>YIELD STRESS</u> (kpsi)
223	5.88	74.35
224	4.94	78.84
225	4.61	81.87
234	12.83	78.64
266	21.47	74.83
<u>Value of the material parameter 'n' = 35.5</u>		
245	12.10	76.02
257	27.73	73.77
258	25.85	75.67
267	18.11	77.65
<u>Value of the material parameter 'n' = 33.0</u>		
215	5.49	75.49
221	7.40	75.30
233	15.45	75.26
243	16.77	74.65
255	39.82	71.04
<u>Value of the material parameter 'n' = 35.0</u>		

TABLE 12

BATCH A

SAMPLE NO.	STRAIN RATE (INCH/INCH/SEC)	YIELD STRESS (KPSI)
115	.447	77.41
116	.466	81.40
118	.433	78.08
123	.389	81.28
124	.544	80.77
132	.198	74.81
136	.190	77.25
137	.229	81.88
143	.123	74.46
144	.169	75.79
145	.196	80.49
146	.226	80.22
152	.062	76.77
154	.060	70.75
155	.070	74.93
156	.077	75.59
159	.095	73.49
164	.089	75.23
165	.100	76.18
166	.118	76.13
167	.135	79.66

SLOPE OF LOG-LOG CURVE = 25.2

VALUE OF THE MATERIAL PARAMETER 'n' = 24.2

TABLE 13

BATCH B

SAMPLE NO.	STRAIN RATE (INCH/INCH/SEC)	YIELD STRESS (KPSI)
215	.453	75.49
221	.335	75.30
223	.417	74.35
224	.526	78.84
225	.583	81.47
233	.158	75.26
234	.199	78.64
243	.144	74.65
245	.204	76.02
255	.058	71.04
257	.086	73.77
258	.095	75.67
266	.113	74.83
267	.139	77.65

SLOPE OF LOG-LOG CURVE = 34.1

VALUE OF THE MATERIAL PARAMETER 'n' = 33.1

## BATCH A

SAMPLE NO.	PULSE DURATION	FORM FUNCTION	FLOW FUNCTION
111	12.57	1.66E-01	1.56E+40
112	12.76	2.33E-01	1.59E+41
113	12.79	2.17E-01	2.10E+42
114	12.94	1.84E-01	1.08E+43
115	13.00	1.32E-01	4.75E+43
116	12.80	1.29E-01	1.46E+44
117	13.01	1.79E-01	3.07E+43
118	13.03	1.40E-01	6.17E+43
121	15.84	1.82E-01	1.25E+43
122	16.67	1.53E-01	5.08E+43
123	16.75	7.41E-02	1.06E+44
124	17.22	7.08E-02	8.99E+43
125	17.70	8.03E-02	5.12E+44
131	34.05	1.31E-01	3.73E+43
132	33.51	7.08E-01	3.00E+44
133	32.25	2.90E-01	7.78E+43
134	32.16	1.53E-01	1.41E+43
135	31.94	1.61E-01	3.41E+42
136	32.36	9.51E-02	8.15E+43
137	32.48	1.04E-01	3.43E+44
141	41.40	1.44E-01	5.81E+42
142	40.89	1.52E-01	2.87E+43
143	40.69	1.13E-01	5.23E+43
144	41.55	1.14E-01	8.09E+43
145	40.20	1.33E-01	3.63E+44
146	40.62	3.42E-01	8.74E+44
147	40.12	1.60E-01	1.50E+43
148	40.32	1.59E-01	1.80E+43
151	89.14	1.53E-01	4.41E+43
152	89.76	9.56E-02	2.03E+44
153	89.73	1.52E-01	1.91E+43
154	90.95	9.85E-02	3.14E+43
155	89.49	1.09E-01	1.29E+44
156	90.38	1.08E-01	1.57E+44
157	90.64	1.61E-01	4.08E+42
158	89.44	1.58E-01	1.33E+43
159	90.10	8.93E-01	6.77E+44
161	62.53	1.68E-01	1.20E+43
162	62.43	1.68E-01	2.99E+43
163	62.04	1.34E-01	4.38E+43
164	62.70	9.93E-02	8.97E+43
165	62.58	8.02E-02	9.63E+43
166	63.74	1.04E-01	1.26E+44
167	63.84	1.79E-01	6.13E+44
168	62.38	1.33E-01	1.88E+43
169	62.14	1.26E-01	6.39E+43
1610	62.39	1.54E-01	3.05E+43

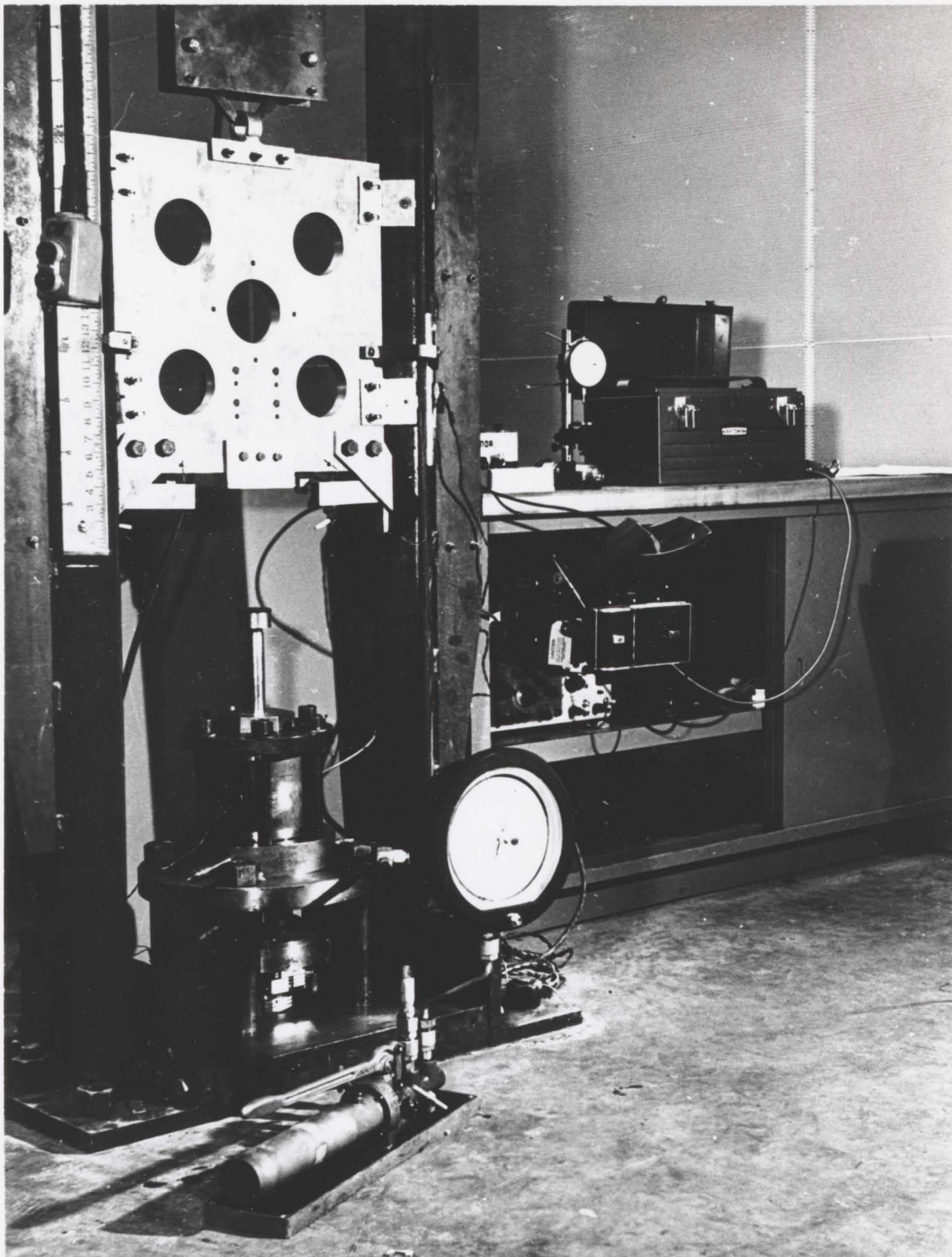
TABLE 15

BATCH B

SAMPLE NO.	PULSE DURATION	FORM FUNCTION	FLOW FUNCTION
211	13.28	1.84E-01	3.41E+60
212	13.81	1.70E-01	3.38E+60
213	14.02	1.66E-01	1.09E+61
214	13.96	1.87E-01	1.59E+61
215	13.60	1.05E-01	1.34E+62
221	18.11	8.18E-02	1.28E+62
222	18.19	1.26E-01	4.81E+61
223	18.75	1.14E-01	1.21E+62
224	18.18	4.68E-02	3.34E+62
225	18.44	7.45E-02	1.59E+63
231	32.42	1.36E-01	3.23E+60
232	32.63	1.25E-01	1.48E+61
233	32.66	8.04E-02	2.23E+62
234	33.18	4.69E-02	5.63E+62
235	33.63	1.32E-01	1.00E+63
241	39.45	1.36E-01	1.17E+61
242	39.58	1.20E-01	1.23E+62
243	39.90	8.38E-02	2.16E+62
244	40.28	1.61E-01	5.10E+62
245	40.33	2.44E-01	1.16E+63
246	40.04	1.18E-01	2.54E+61
251	90.08	1.39E-01	8.39E+60
252	90.70	1.31E-01	1.36E+61
253	89.65	1.24E-01	7.45E+61
254	89.73	1.33E-01	2.26E+61
255	91.04	8.94E-02	1.03E+62
256	91.44	1.49E-01	1.73E+62
257	90.44	1.68E-01	6.69E+62
258	90.78	5.79E-01	5.35E+63
261	62.24	9.84E-02	3.15E+61
262	62.72	1.32E-01	2.87E+61
263	62.66	1.16E-01	5.40E+61
264	62.75	1.26E-01	1.49E+62
265	63.09	9.01E-02	1.13E+62
266	63.82	1.15E-01	5.16E+62
267	63.81	4.19E-01	6.37E+63

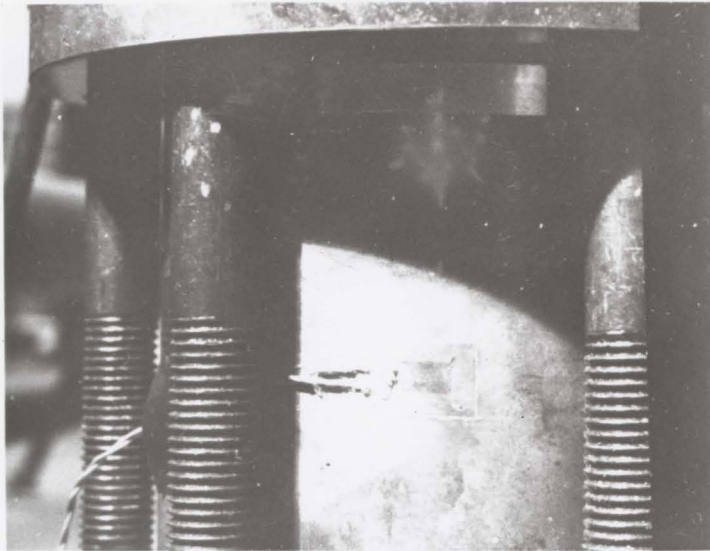
APPENDIX V

FIGURES



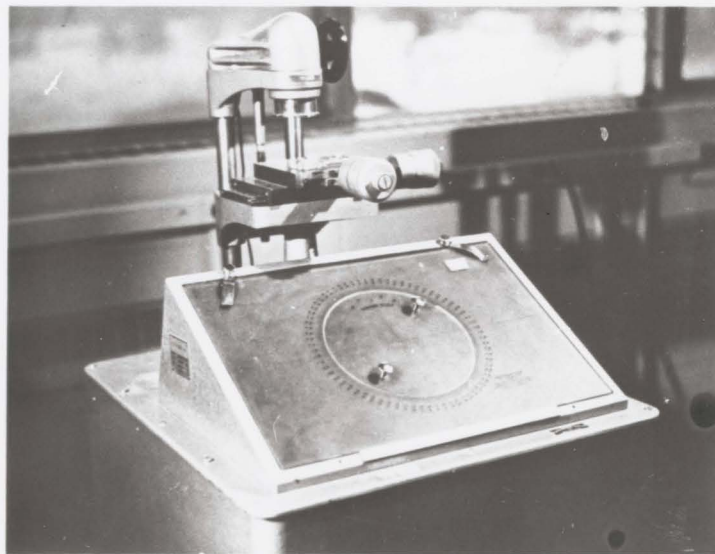
GENERAL VIEW OF THE EXPERIMENTAL SET UP

FIGURE 1



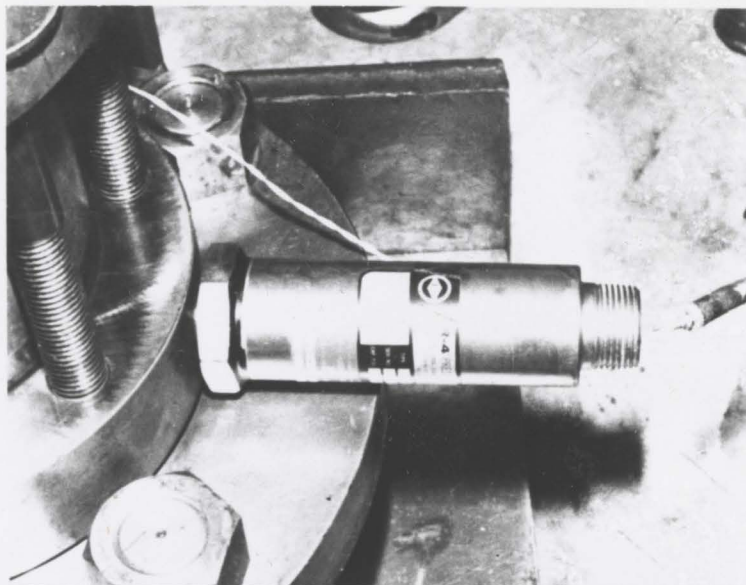
STRAIN GAGE CEMENTED TO THE WALL  
OF THE HYDRAULIC INTENSIFIER

FIGURE 2



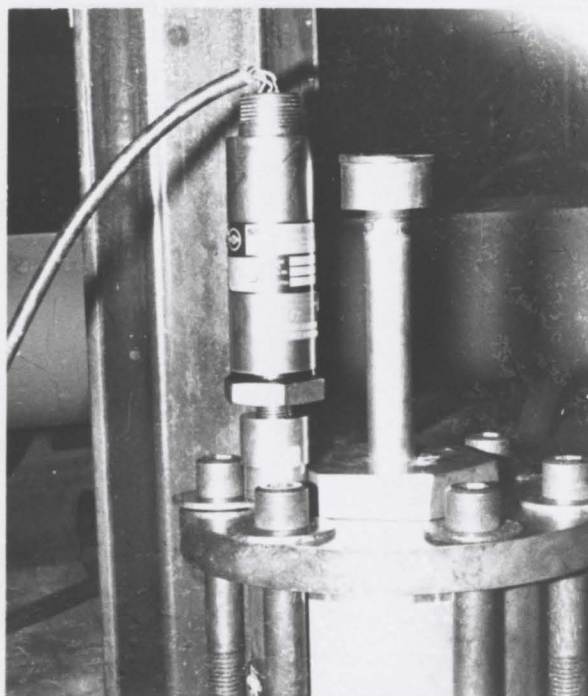
MICRO WILDER PROJECTOR

FIGURE 3



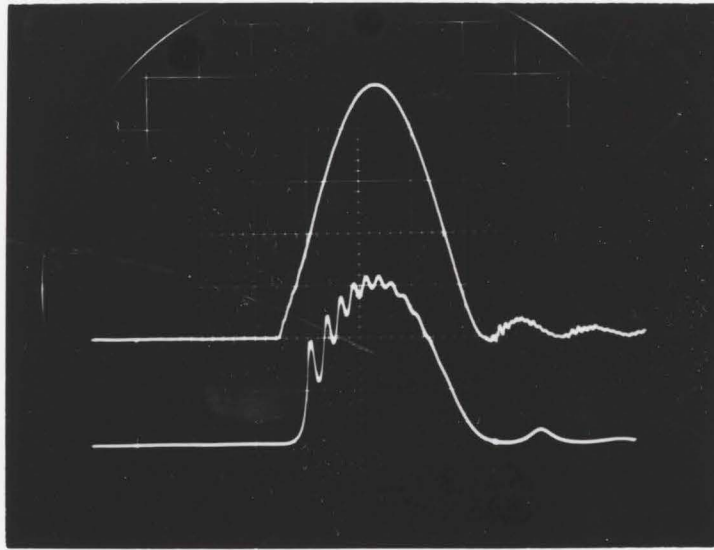
PRESSURE TRANSDUCER CONNECTED TO THE LOWER  
PORTION OF THE INTENSIFIER

FIGURE 4



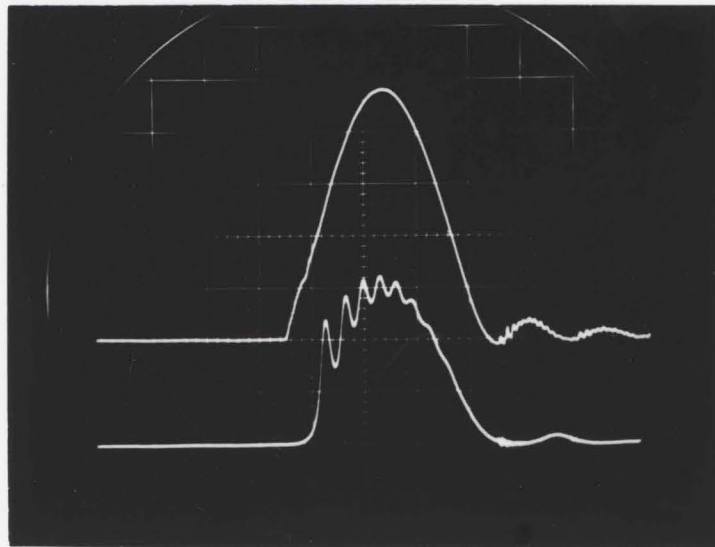
PRESSURE TRANSDUCER CONNECTED TO THE  
INTENSIFIER THROUGH THE AIR-VENT

FIGURE 5



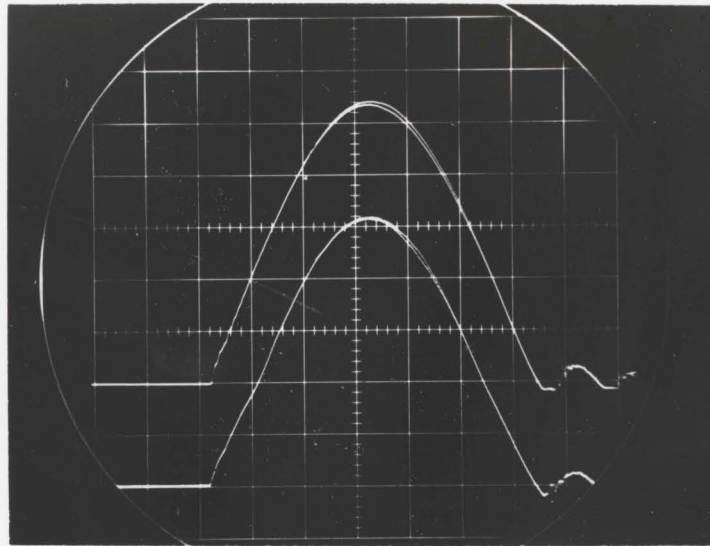
LOWER TRACE IN THE FIGURE IS THE  
PRESSURE PULSE OBTAINED WITH THE  
CONFIGURATION SHOWN IN FIGURE 4

FIGURE 6



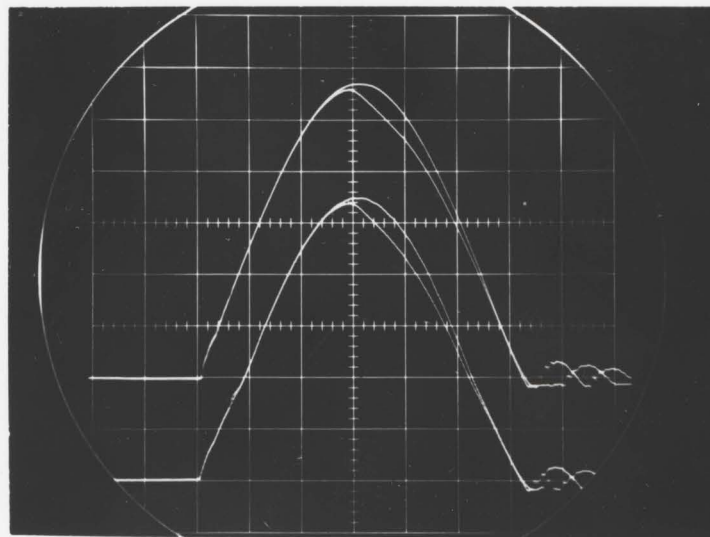
PRESSURE PULSE OBTAINED WITH THE  
CONFIGURATION SHOWN IN FIGURE 5

FIGURE 7



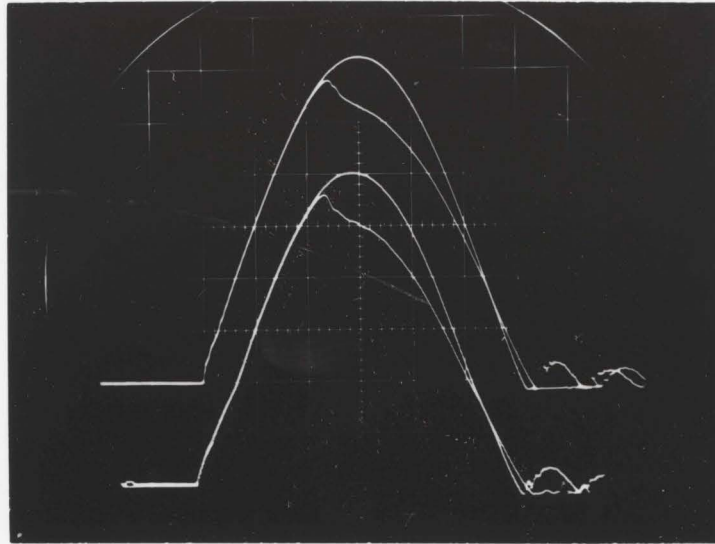
LOAD-TIME TRACE FOR TEST SAMPLE 1610

FIGURE 8



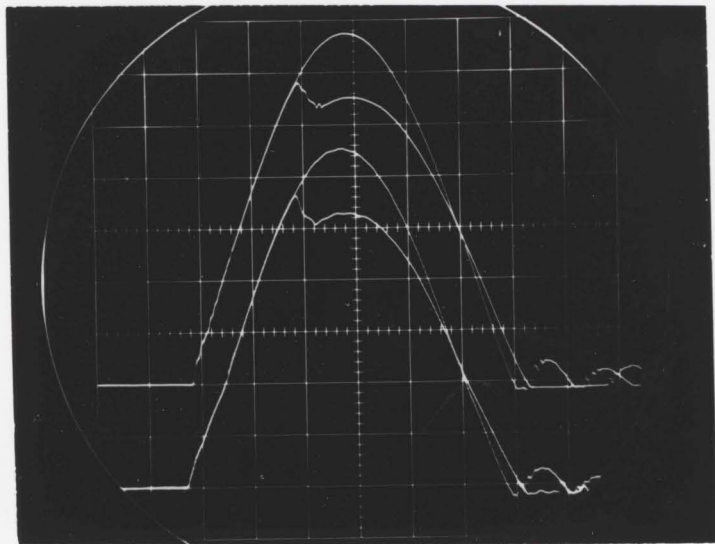
LOAD-TIME TRACE FOR TEST SAMPLE 169

FIGURE 9



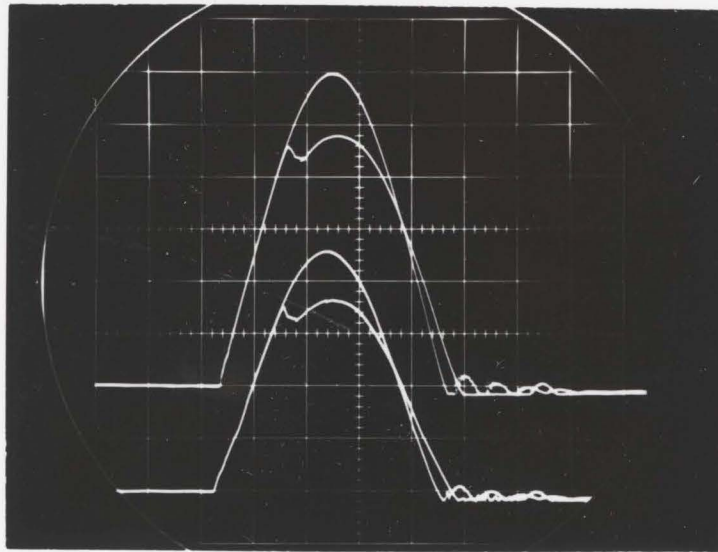
LOAD-TIME TRACE FOR TEST SAMPLE 165

FIGURE 10



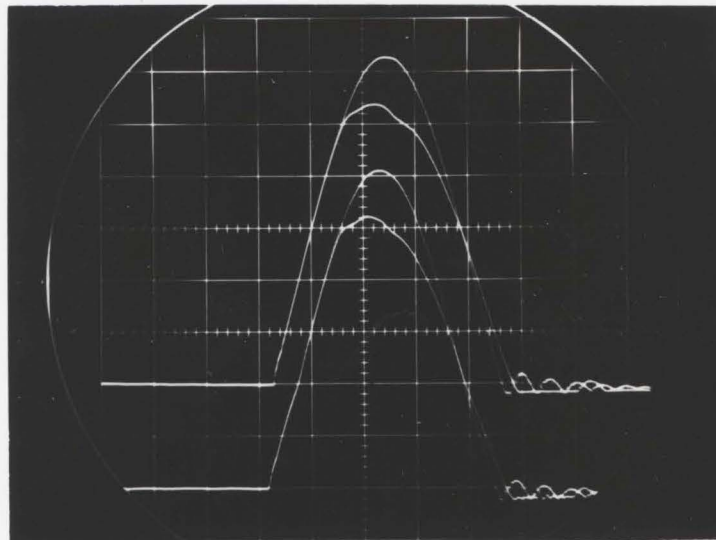
LOAD-TIME TRACE FOR TEST SAMPLE 166

FIGURE 11



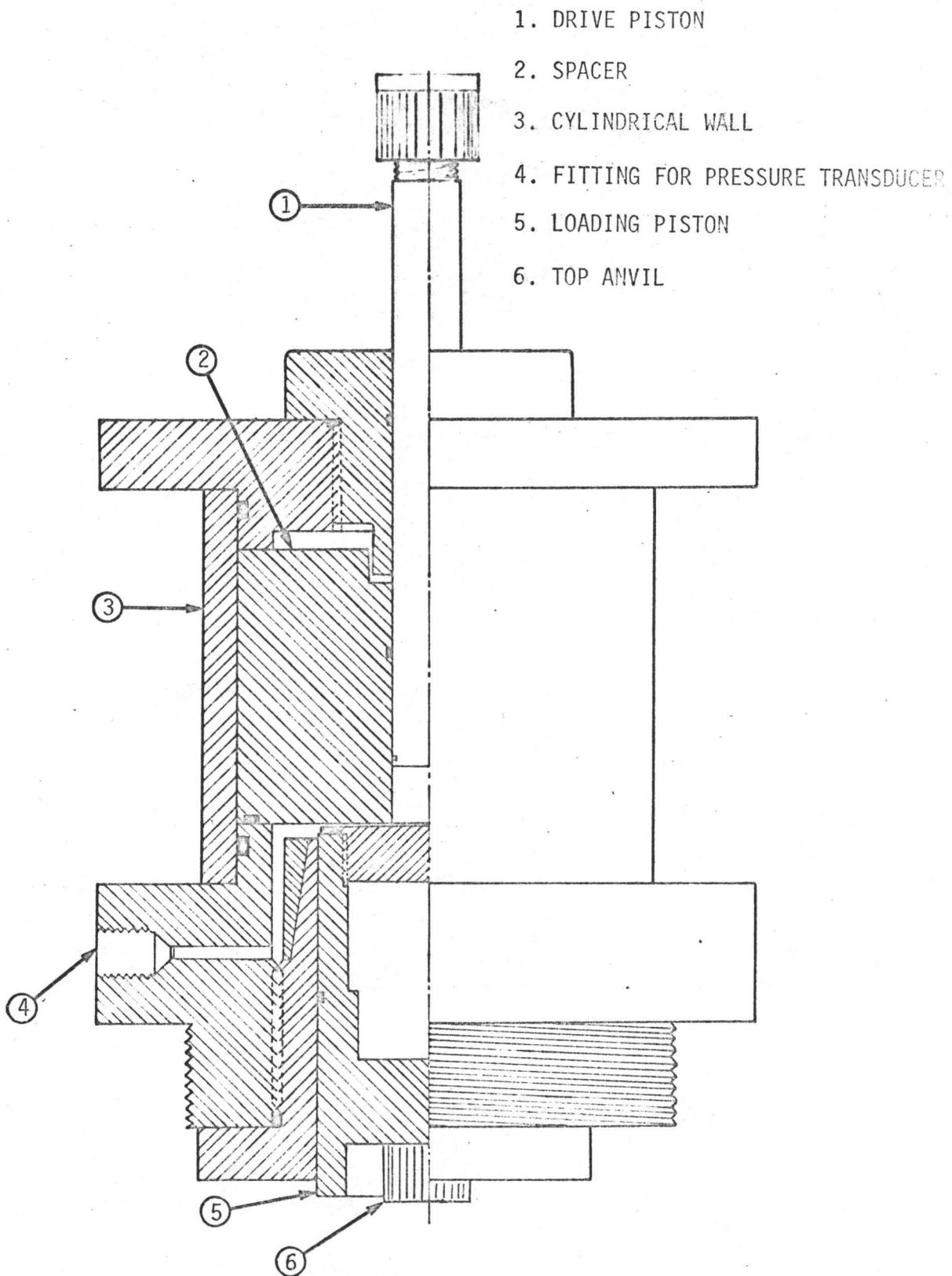
- LOAD-TIME TRACE FOR TEST SAMPLE 258

FIGURE 12



LOAD-TIME TRACE FOR TEST SAMPLE 256

FIGURE 13

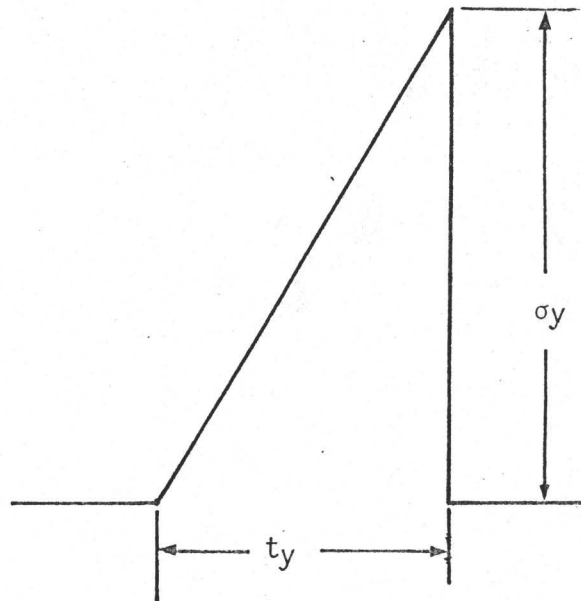


1. DRIVE PISTON
2. SPACER
3. CYLINDRICAL WALL
4. FITTING FOR PRESSURE TRANSDUCER
5. LOADING PISTON
6. TOP ANVIL

SECTIONAL VIEW OF THE HYDRAULIC INTENSIFIER

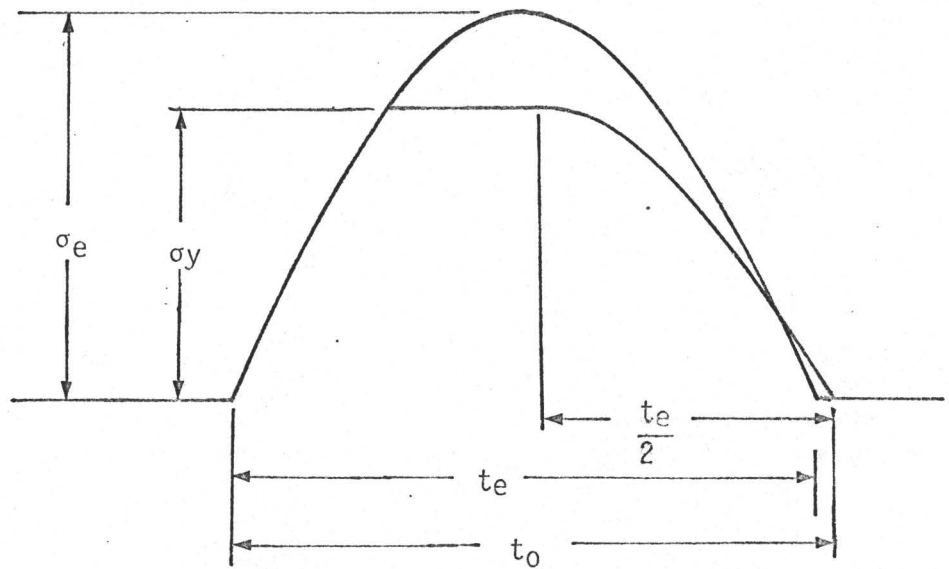
( MORE DETAILS ARE PRESENTED IN REFERENCES 1 AND 2 )

FIGURE 14



STRESS PULSE FOR CONSTANT RATE  
OF LOADING

FIGURE 15



STRESS PULSE FOR AN IDEALLY ELASTIC-PLASTIC MATERIAL

FIGURE 16

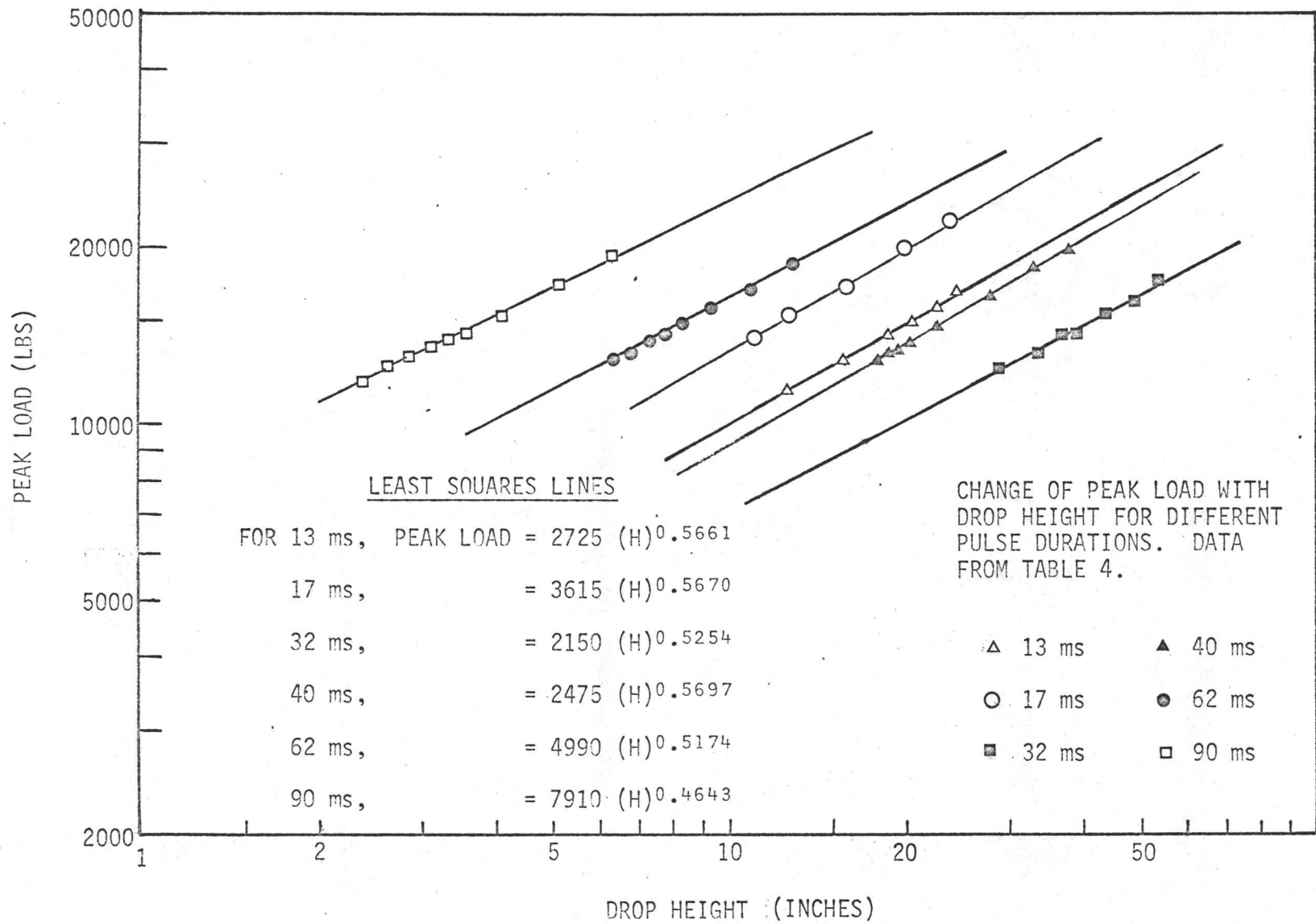


FIGURE 17

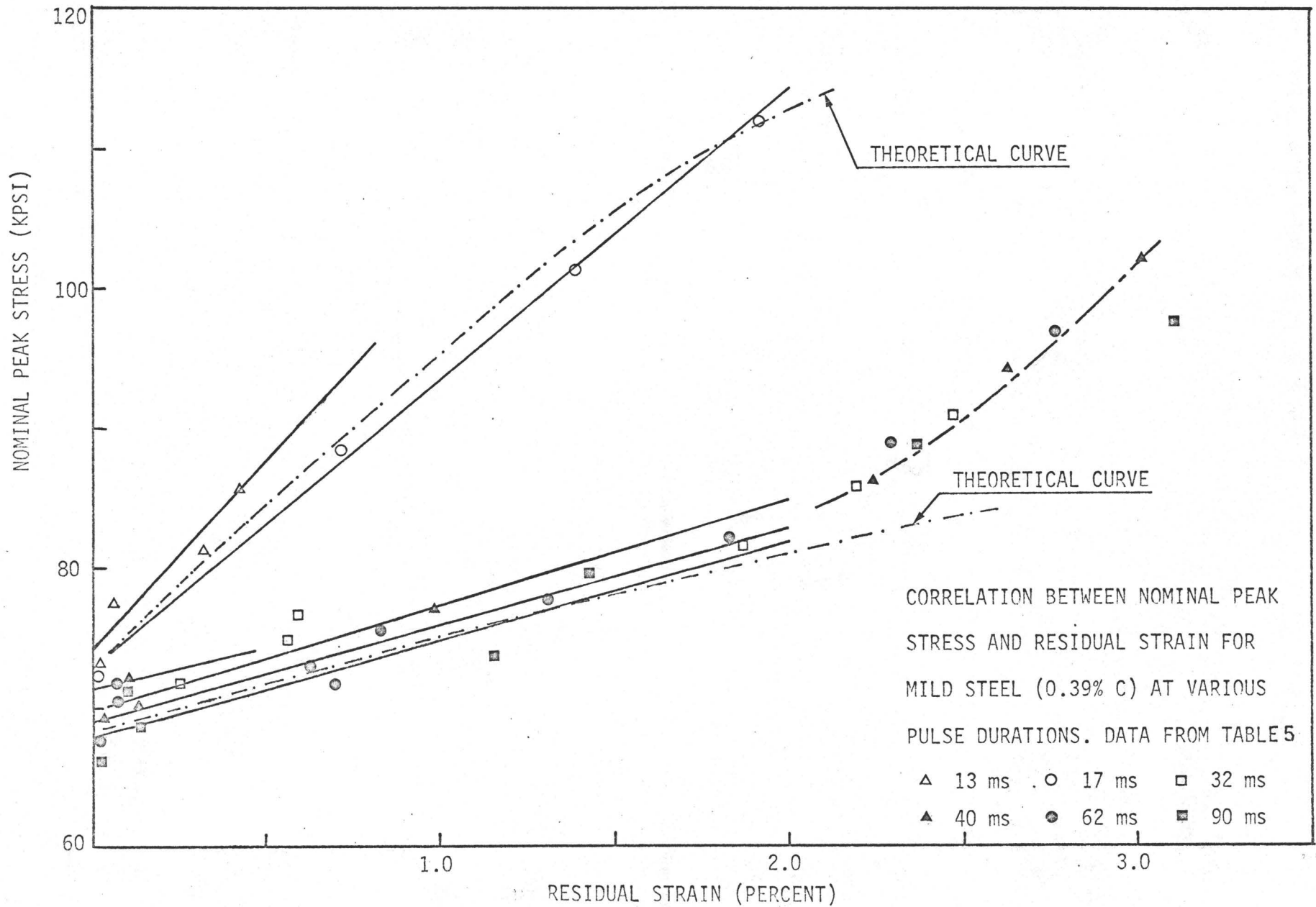


FIGURE 18

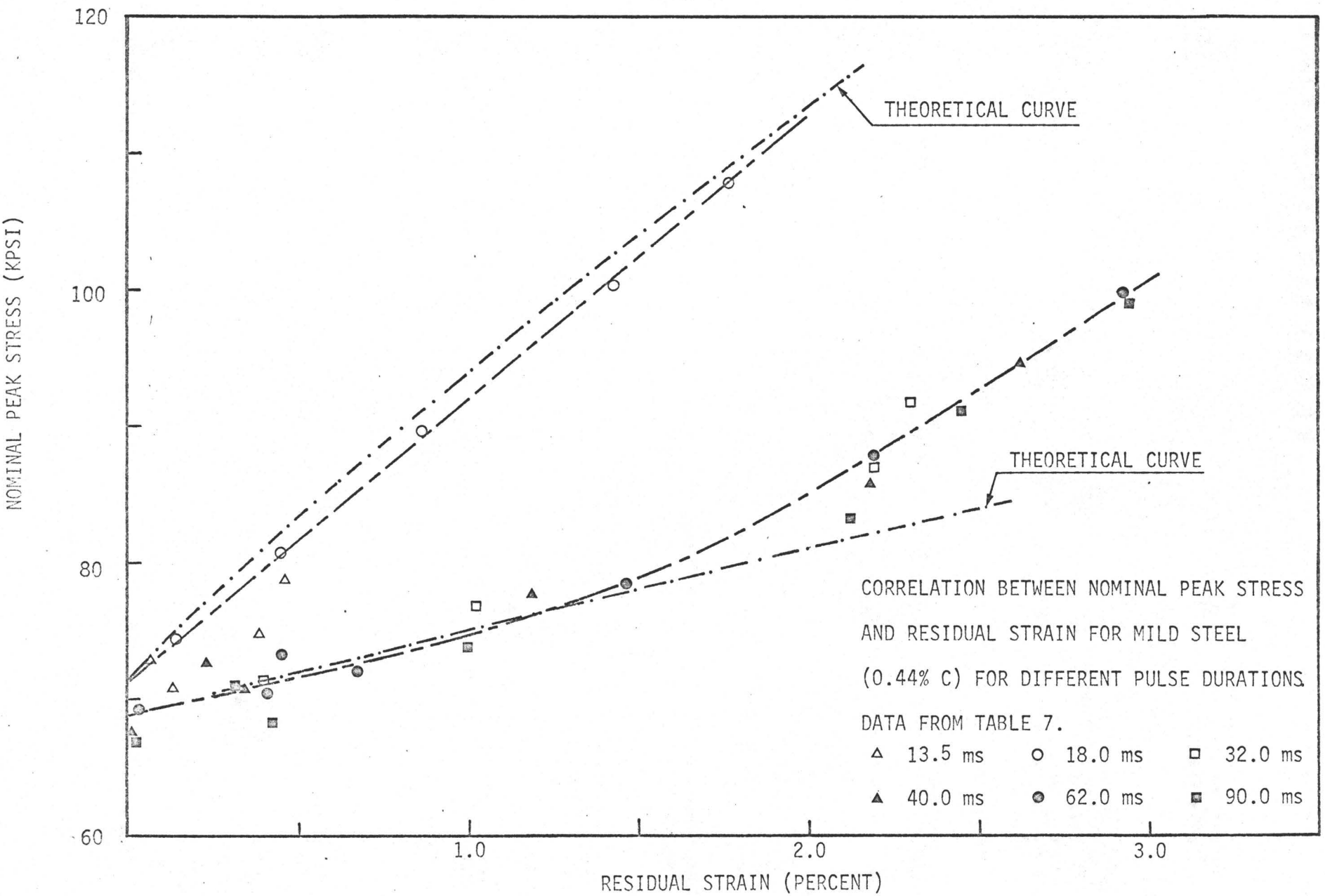


FIGURE 19

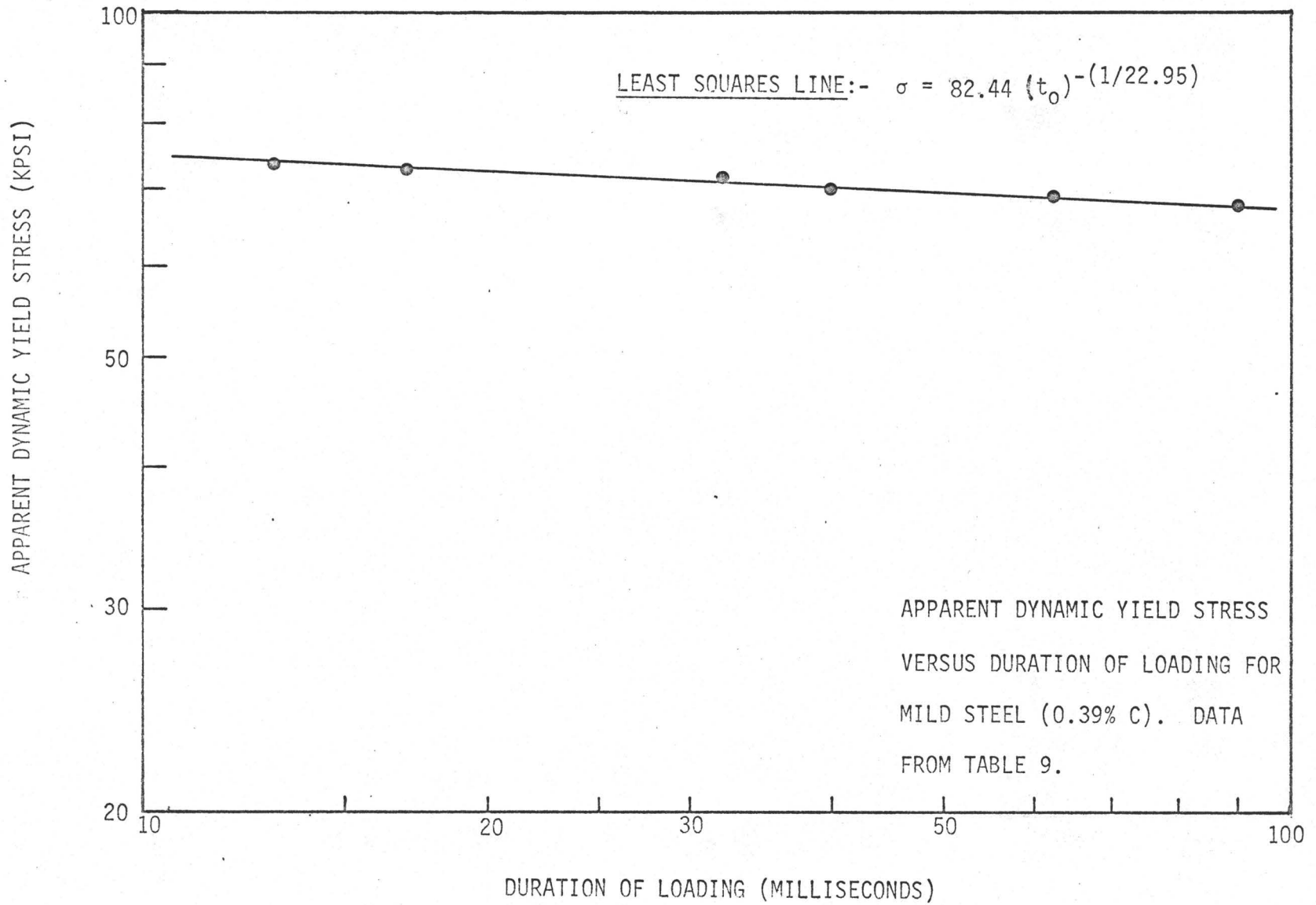


FIGURE 20

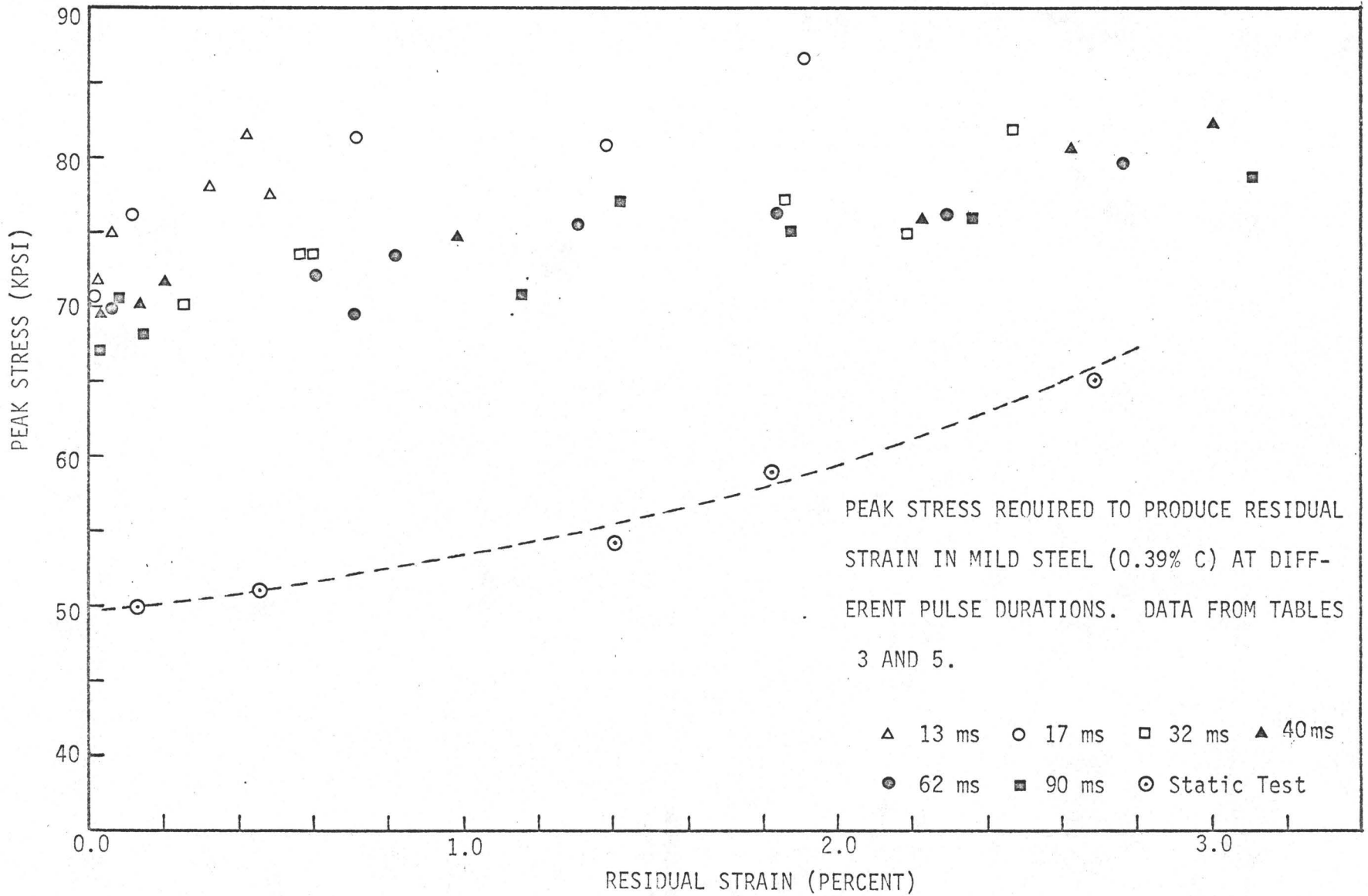


FIGURE 21

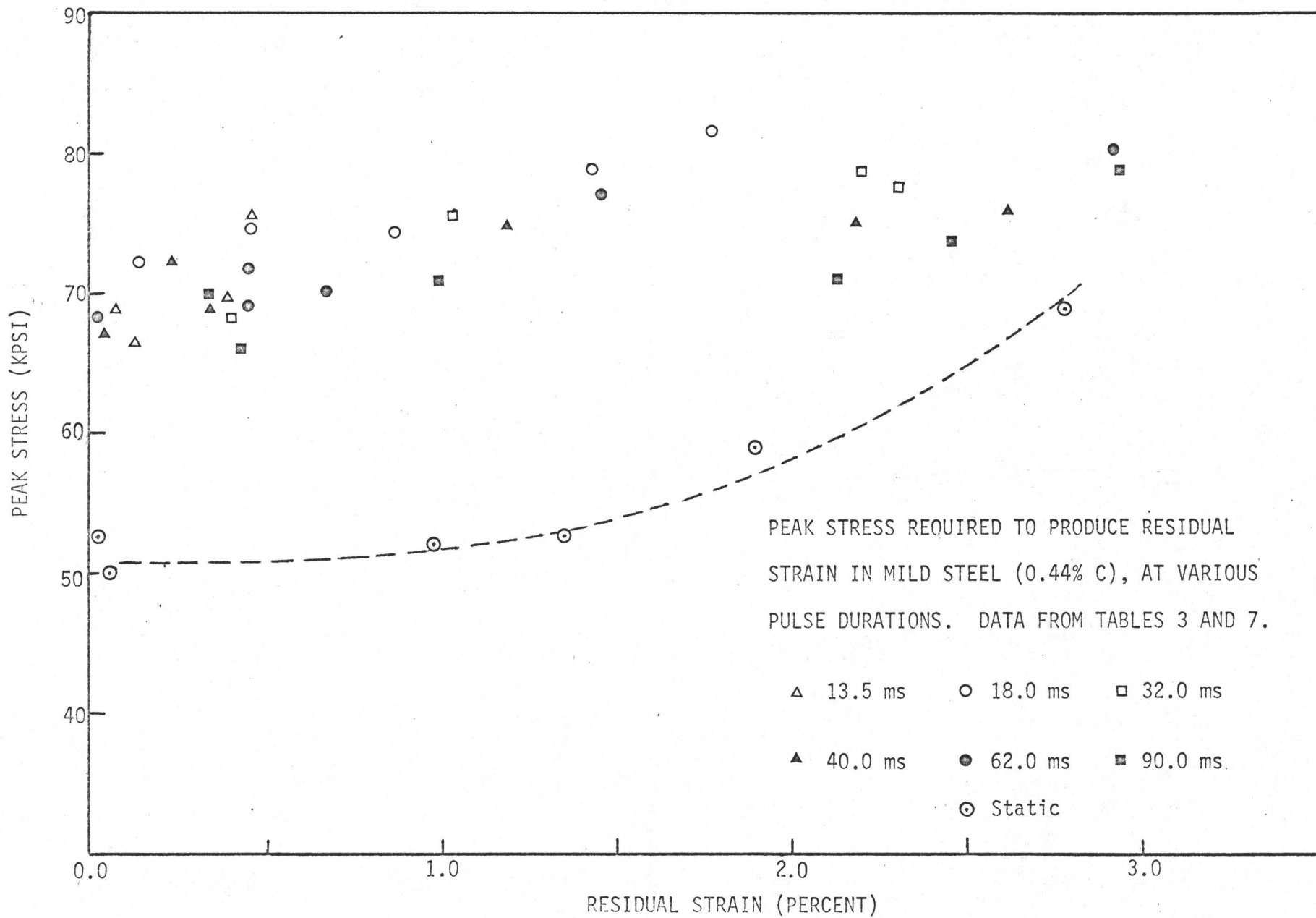


FIGURE 22

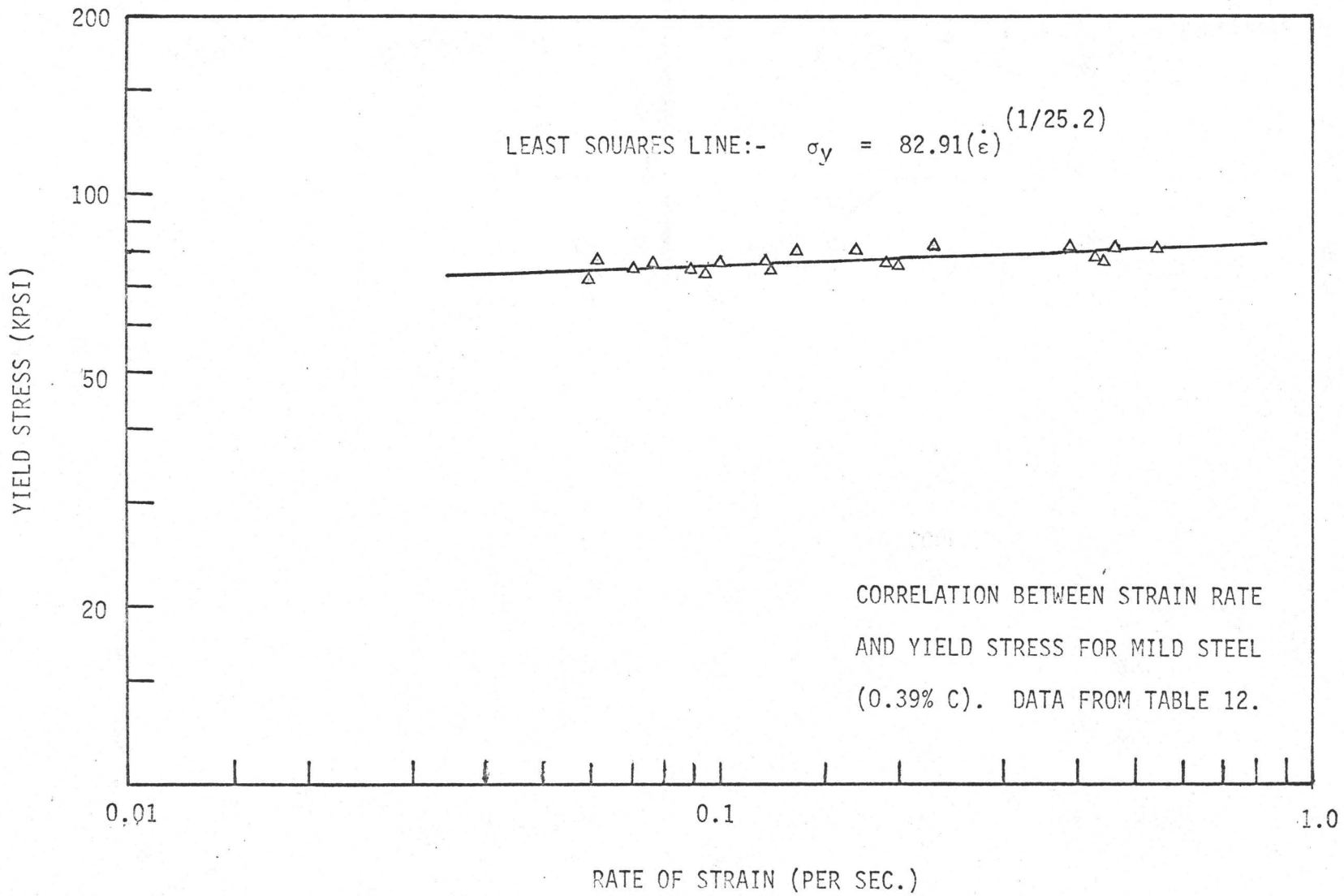


FIGURE 23

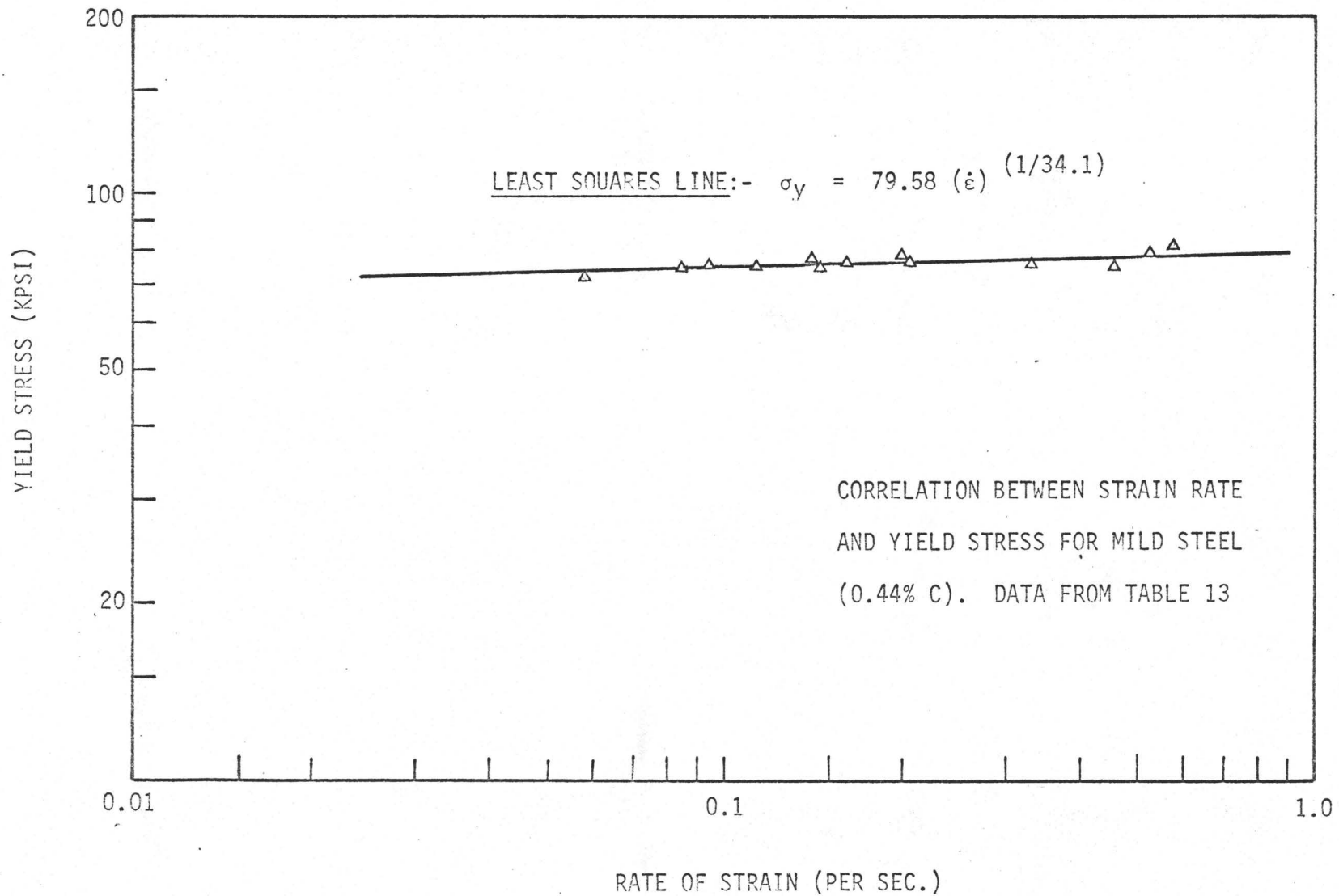


FIGURE 24

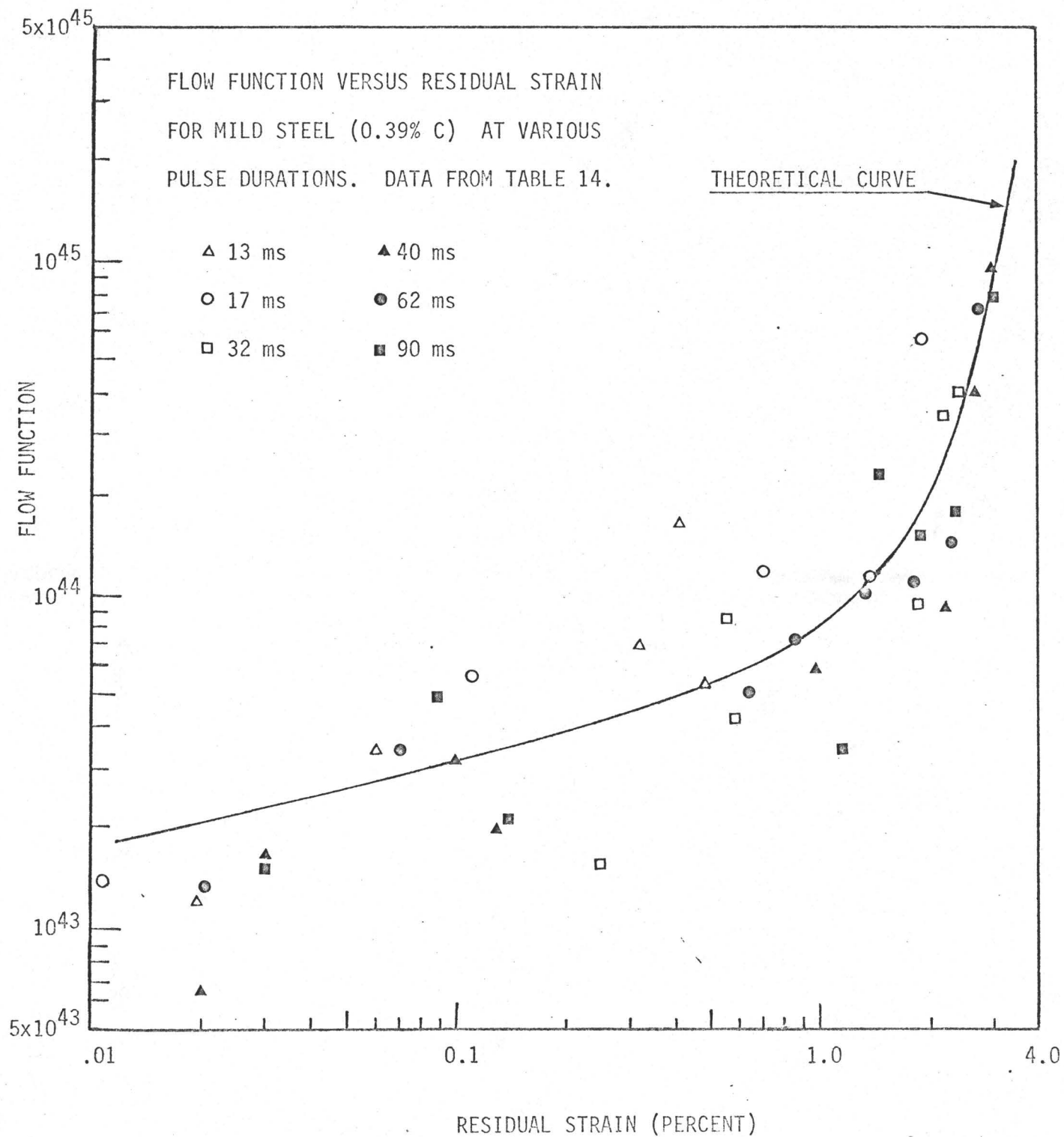


FIGURE 25

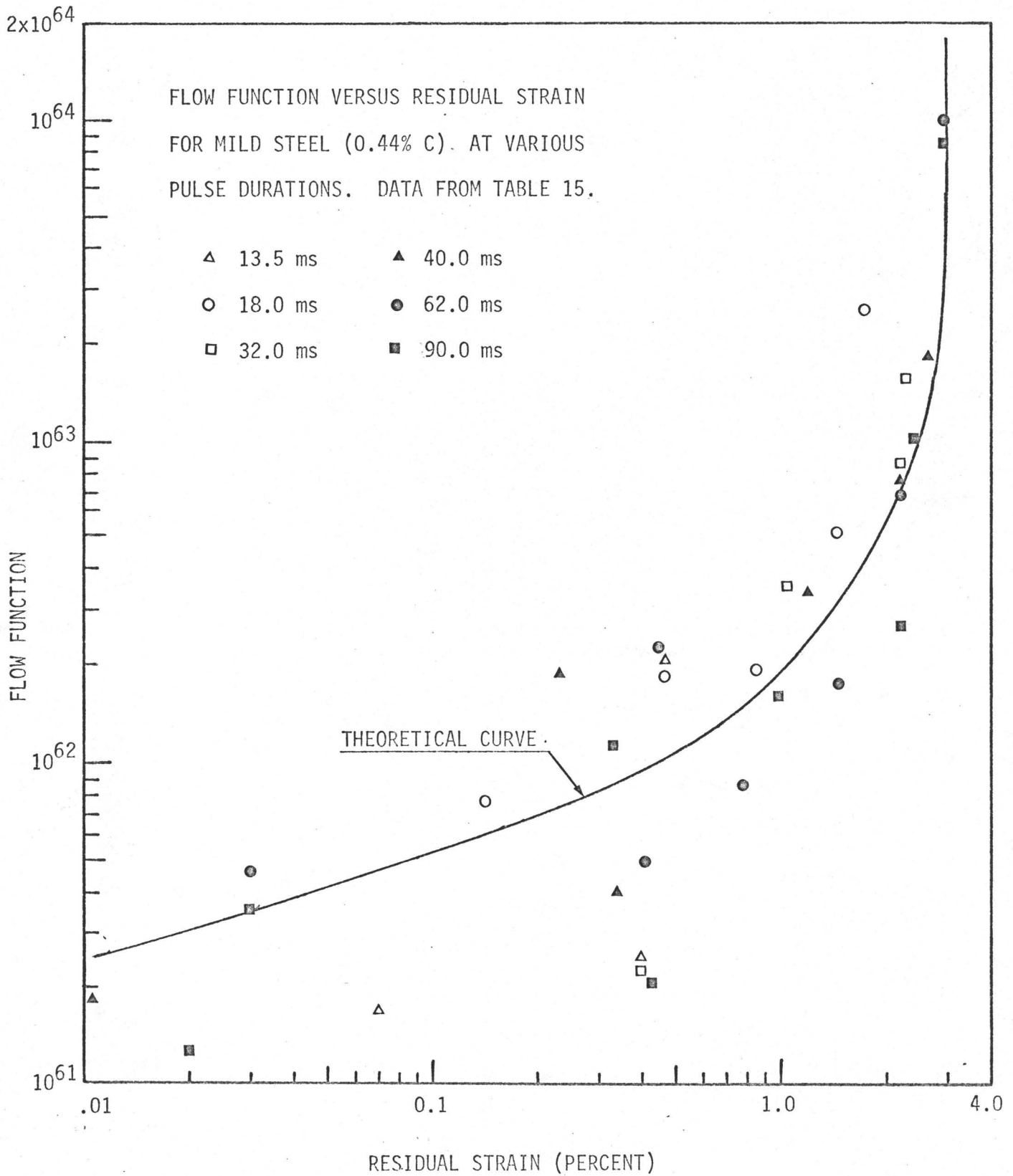


FIGURE 26

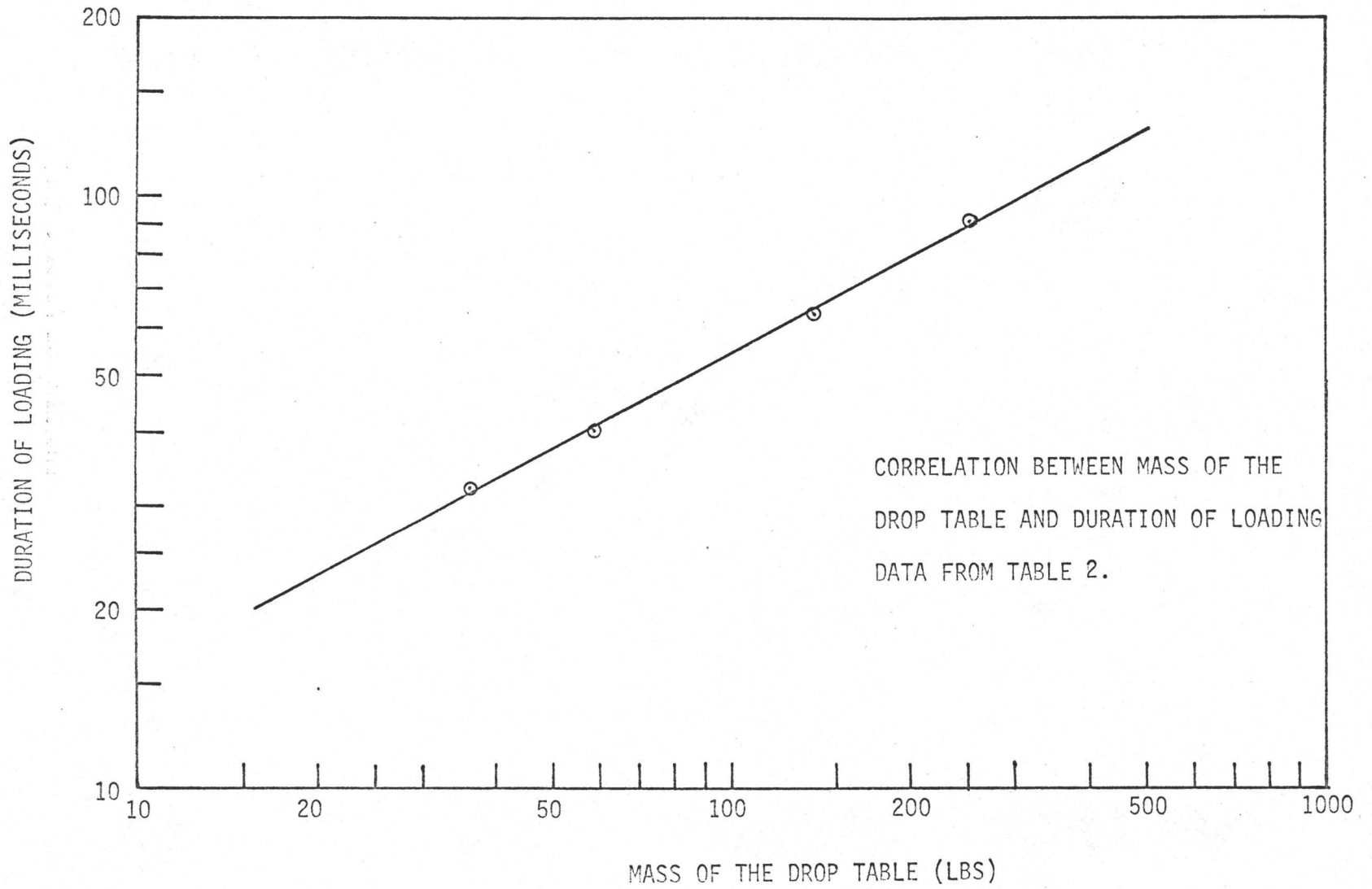


FIGURE 27

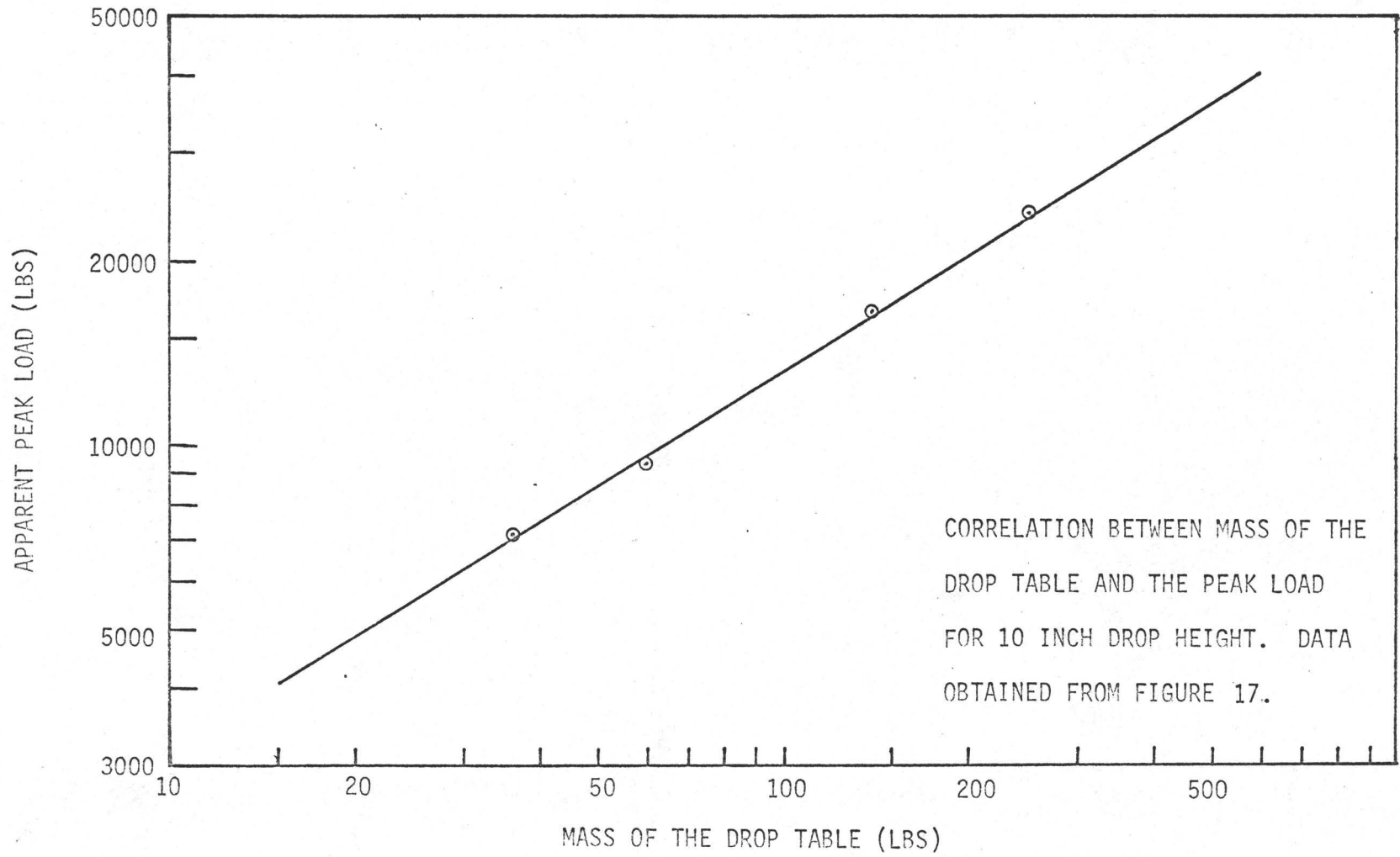


FIGURE 28

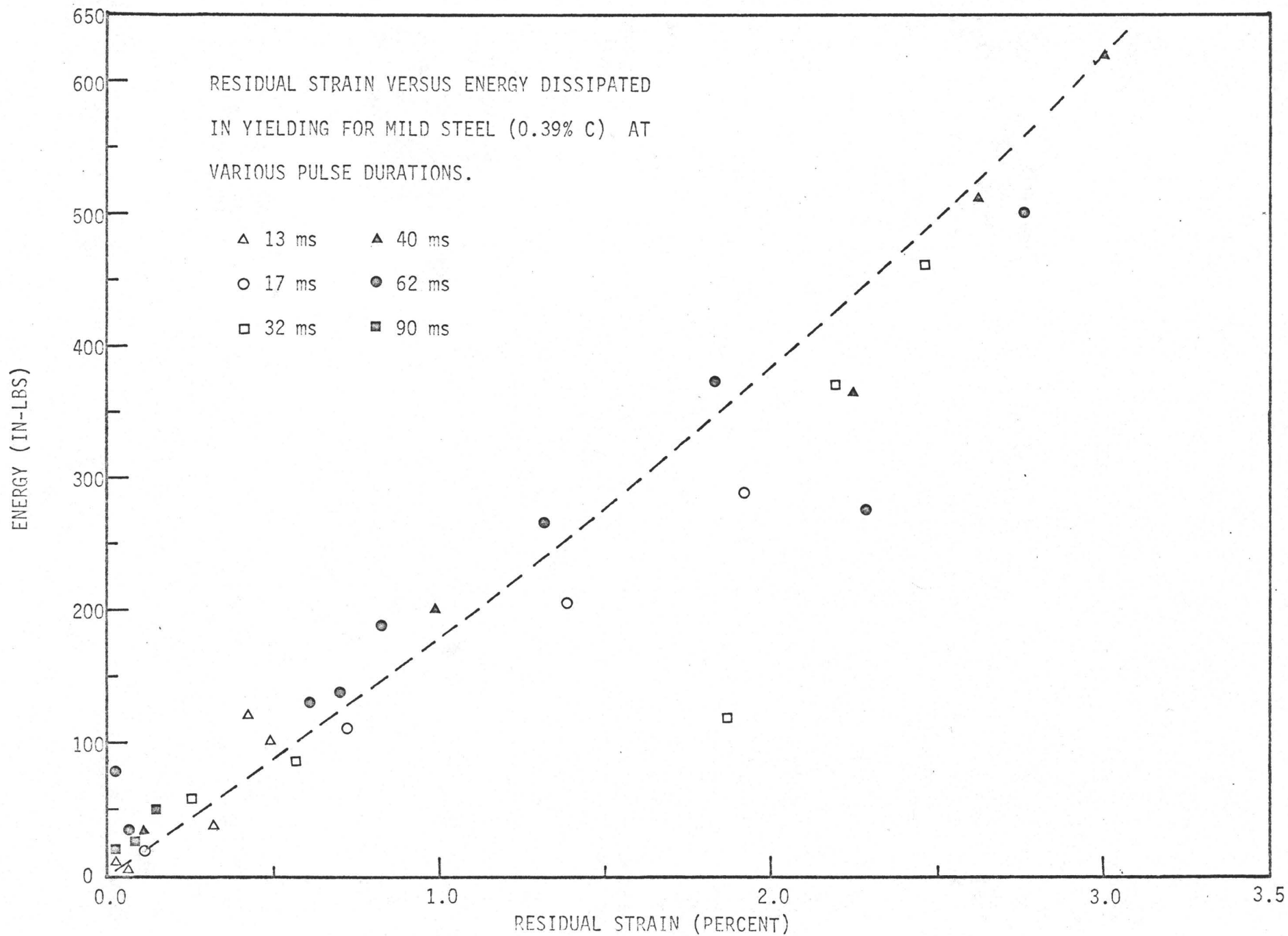


FIGURE 29

99

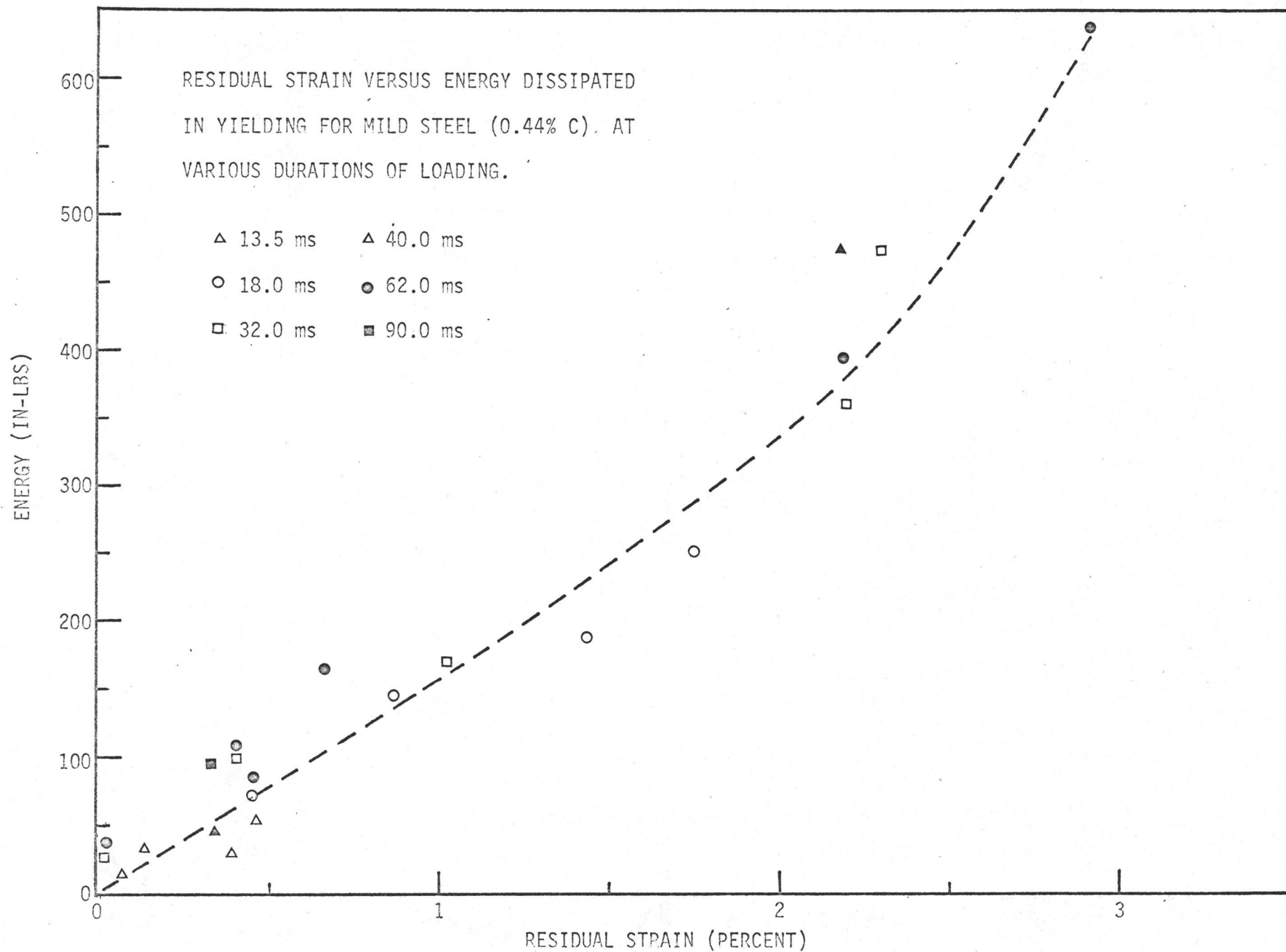


FIGURE 30

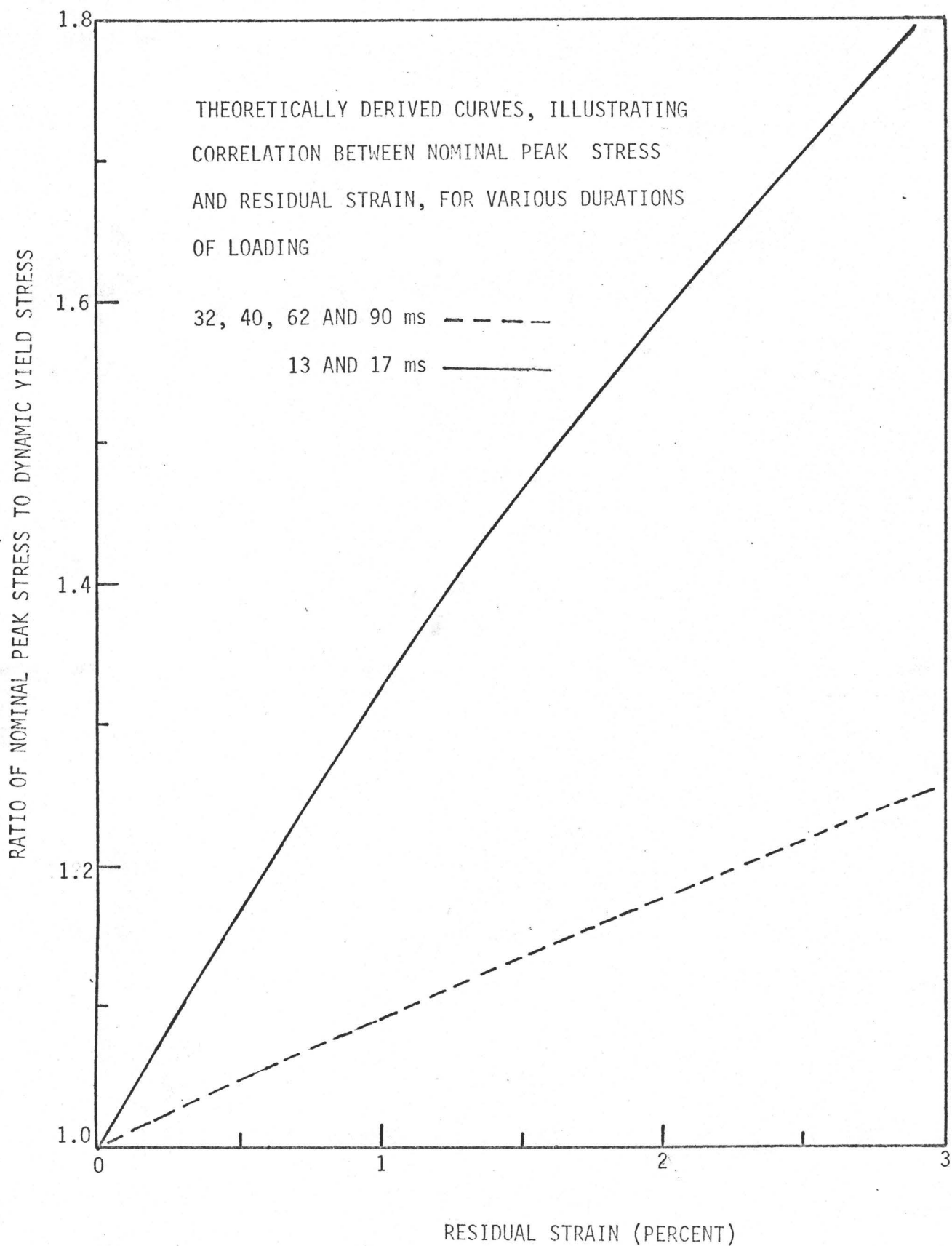


FIGURE 31

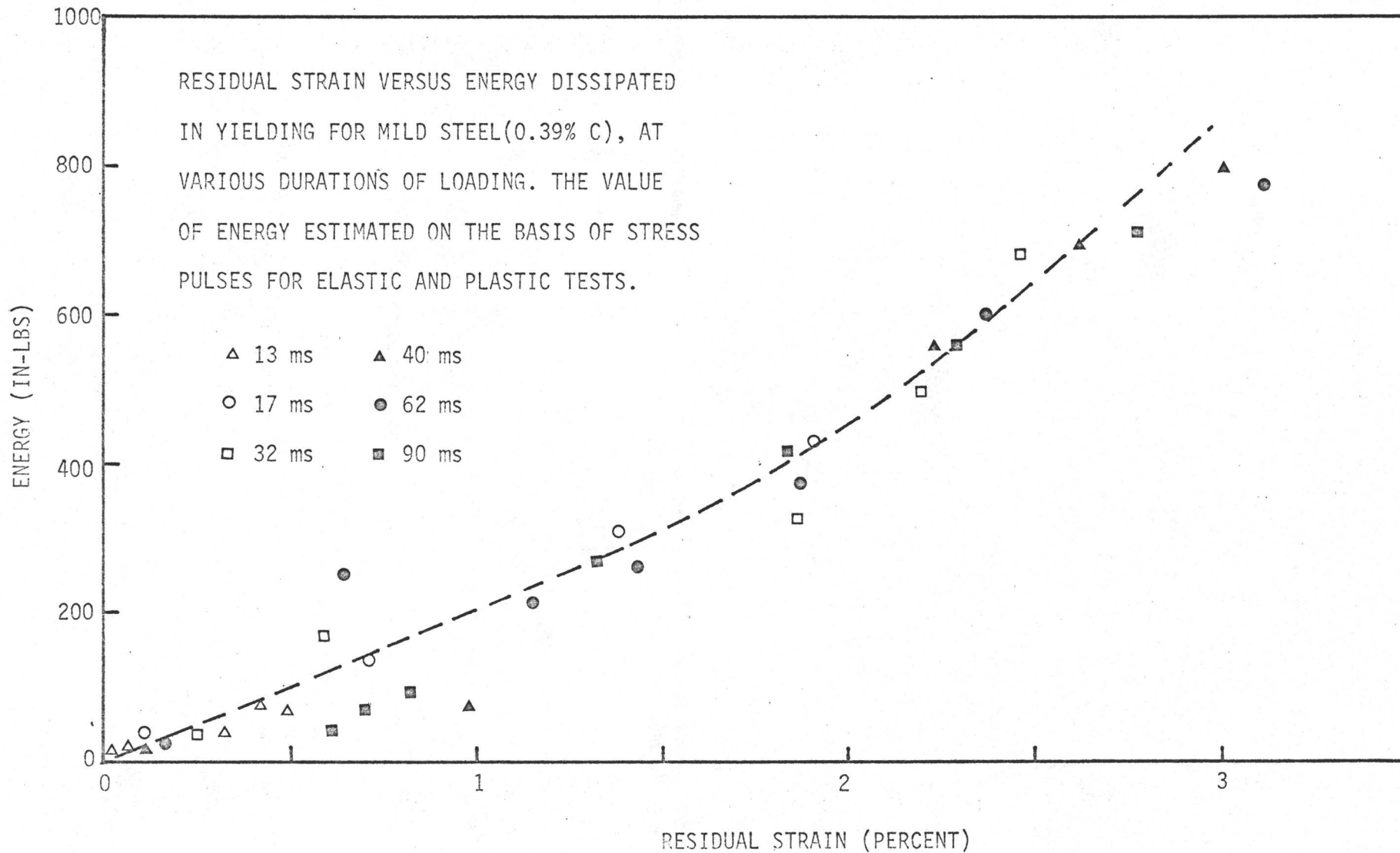


FIGURE 32

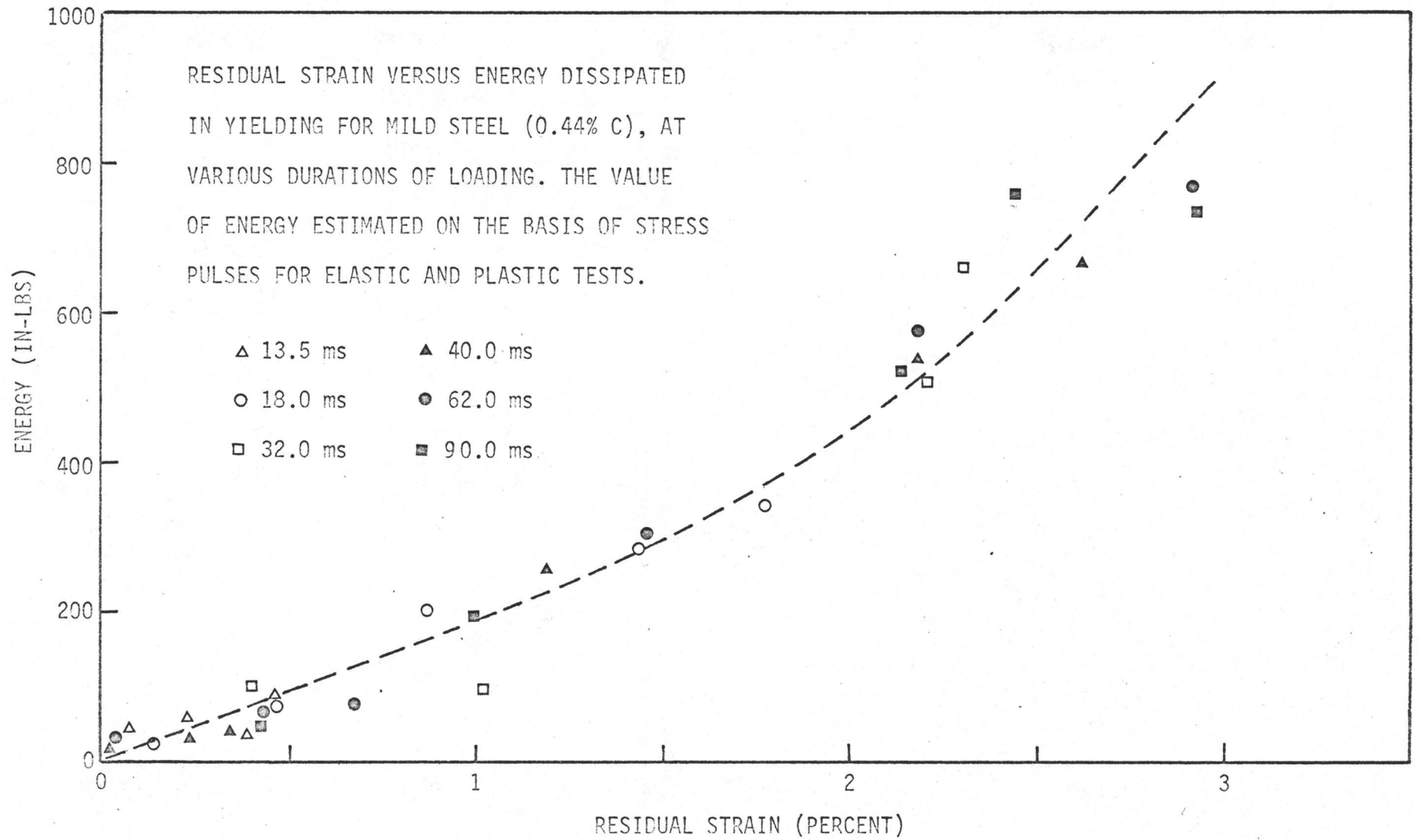


FIGURE 33

## REFERENCES

1. Kardos, G., "A study of Plastic Flow in Steel at High Rates of Strain", Ph.D. thesis, Department of Mechanical Engineering, McGill University, Montreal, Quebec, 1965.
2. Sinha, S.K., "Plastic Strain in Materials Under the influence of Impulsive Load", M. Eng. thesis, Department of Mechanical Engineering, McMaster University, Hamilton, Ontario, 1968.
3. Hopkinson, B., "On the Rupture of Iron Wire by a Blow", Proceedings of the Royal Society A74(1905), 498.
4. Hahn, G.T., "A Model for Yielding with Special Reference to the Yield-Point Phenomena of Iron and Related B.C.C Metals", Acta Metallurgica, Vol. 10, Aug. 1962.
5. Campbell, J.D., "The Dynamic Yielding of Mild Steel", Acta Metallurgica, Vol. 1, 1963.
6. Hull, D. and Noble, F., "Indirect Measurement of the Effect of Stress on the Velocity of Dislocations", Faraday Society, 1964 (preprint)
7. Clark, D.S. and Wood, D.S., "Time Delay for the Initiation of Plastic Deformation of Rapidly Applied Constant Stress", Proceedings ASTM Vol. 49, 1949.
8. Biggs, N.D., "The Brittle Fracture of Steel", Chapter IV, Macdonal & Evans Ltd.
9. Kardos, G., "Response of Metals to High Strain Rates-a Review of the Literature", Mechanical Engineering Faculty, McGill University, Rev. 64-1, May 1964.